IMPACT OF SIMULATED MITRACLIP ON FORWARD FLOW OBSTRUCTION IN THE SETTING OF MITRAL LEAFLET TETHERING

A Dissertation
Presented to
The Academic Faculty

by

Charles H. Bloodworth IV

In Partial Fulfillment
of the Requirements for the Degree
Master of Science in Bioengineering in the
George W. Woodruff School of Mechanical Engineering

Georgia Institute of Technology
December, 2017

IMPACT OF SIMULATED MITRACLIP ON FORWARD FLOW OBSTRUCTION IN THE SETTING OF MITRAL LEAFLET TETHERING

Approved by:

Dr. Ajit P. Yoganathan, Advisor
Department of Biomedical Engineering
Georgia Institute of Technology

Dr. Vasilis C. Babaliaros
Department of Medicine
Emory University

Dr. Rudolph L. Gleason
School of Mechanical Engineering
Georgia Institute of Technology

Date Approved: September 22nd, 2017

To hard work and perseverance

ACKNOWLEDGEMENTS

I would first like to thank my academic collaborators for their input and support. This work would not have been possible without critical clinical guidance from Dr. Vasilis Babaliaros and Dr. Nori Kamioka, and critical engineering guidance provided by Dr. Rudy Gleason.

Second, I would like to thank my undergraduate researchers, Nancy Deaton, Kaitlin Jones and Radhika Duvvuri. You took on challenges, brought ideas to the table and made things happen.

Next, I would like to thank the members of the Cardiovascular Fluid Mechanics research group at Georgia Tech, past and present, not only for their critical feedback to this work, but also for their camaraderie, friendship and perspective. I would like to especially recognize the guidance and opportunity provided by Dr. Ajit Yoganathan. Research as a part of the CFM lab family has been a formative and unforgettable part of my life, and I am beyond thankful for your mentorship over the last four years.

Finally, I would like to thank my family. I wouldn't be here without the support from my mother and father, brother and sister, and my close family members in the Atlanta area. Heather, I truly couldn't have done this without your love, support and encouragement each step of the way.

TABLE OF CONTENTS

LIST OF TABLES

LIST OF FIGURES

LIST OF SYMBOLS AND ABBREVIATIONS

AML	Anterior Mitral Leaflet
DMR	Degenerative Mitral Regurgitation
FMR	Functional Mitral Regurgitation
GLM	General Linear Model
GTclip	Georgia Tech edge-to-edge repair clip
IFU	Indications For Use
LA	Left Atrium
LV	Left Ventricle
MAA	Mitral Annular Area
MR	Mitral Regurgitation
MS	Mitral Stenosis
MV	Mitral Valve
MVA	Mitral Valve Area (by planimetry)
MVG	Mitral Valve pressure Gradient
PM	Papillary Muscle

CHAPTER 1: SUMMARY

In the early 2000s, a catheter-based device known as the Evalve was designed to clip the mitral valve (MV) leaflets together at the site of mitral regurgitation (MR), treating MR without requiring open-heart surgery. This device is now known as MitraClip (Abbott Vascular, Santa Clara, CA), and, with over 45,000 patients treated worldwide, it is currently the only widely-used and FDA approved transcatheter mitral repair device.

MitraClip is a catheter-delivered device designed to grasp and approximate the mitral leaflets, closing the regurgitant orifice and treating MR. MR reduction to <2+ is critical to achieve optimal patient outcomes, and additional clips may be deployed to reach this level of MR reduction. However, by nature, the device also reduces MV Area (MVA) and may increase mean MV gradient (MVG). These two metrics are the key descriptors of Mitral Stenosis (MS), according to clinical guidelines. Indeed, a limitation of MitraClip treatment is the undesirable creation of MS. Recently published clinical reports have shown that significantly poorer long-term patient outcomes result when a patient is left with a mean MVG above 5 mmHg. When treating MR with MitraClip, the benefits of MR reduction must be balanced with concomitant risk of increased MS severity as additional clips are implanted. A “compromise” between complete elimination of MR and significant reduction of MVA due to placement of additional clips may occur, resulting in an aborted clip strategy.

Limited clinical evidence has suggested that, under certain conditions, severity of MS after MitraClip may be further exacerbated by diastolic restriction of the anterior mitral leaflet (AML) caused by severe dilatation of the left ventricle (LV) and papillary muscle

(PM) displacement. This LV remodeling is characteristic of functional mitral regurgitation (FMR). MitraClip is currently not approved in the US for treatment of FMR, but, only in degenerative mitral regurgitation (DMR). However, due to lack of other treatment options, MitraClip is widely-used off-label for treatment of FMR.

The purpose of this study was to determine the conditions under which MitraClip may create Mitral Stenosis (MS) in the setting of AML tethering. Using the Georgia Tech left heart simulator, MitraClip placement was simulated using a custom clip (GTclip) with dimensions identical to MitraClip. One or two GTclips were placed in common locations on excised ovine MV samples (N=6), and AML tethering severity was varied from mild to severe for each of the GTclip placements. Mitral annular area (MAA) was varied for each MV sample, from 3.6 cm^2 to 4.8 cm^2.

AML tethering severity was found to be a highly significant factor increasing MVG and decreasing MVA ($p<0.001$). When GTclip placement was simulated in the presence of severe AML tethering, mean MVG>5mmHg resulted more frequently than with GTclip placement alone (46% v. 4%, respectively). However, at MAA above 4.7 cm^2, severe AML tethering did not cause moderate MS (placement of up to two GTclips, 95% confidence). Here, baseline MVA was near the established minimum for MitraClip treatment ($3.9\pm0.3cm^2$). This first-of-its-kind study will provide valuable information on MitraClip performance, aiding cardiologists patient selection and in determining the suitability of different MitraClip treatments for the large population of FMR patients.

CHAPTER 2: BACKGROUND AND INTRODUCTION

2.1 Valvular Disease and Mitral Regurgitation

Valvular heart disease (VHD) is estimated to affect 2.5% of the population in industrialized countries, and the prevalence of VHD increases drastically in elderly populations.[1] Mitral regurgitation (MR) is the most common valvular disease; moderate levels of MR are found in 6.4% of the population between 65 and 74 years of age, and 9.3% of the population over 75 years of age.[2]

MR can be subdivided into two main categories; degenerative MR (DMR) is a disease of the tissue of the mitral valve (MV) itself, while functional MR (FMR) is a secondary effect of a disease in the left ventricle (LV) or surroundings of the MV.[3] In FMR, remodeling of the papillary muscles (PMs) and mitral annulus cause MV insufficiency.[4] Though the geometric distortions vary widely, PM displacement, annular dilatation, and leaflet tethering are widely accepted as the causes of FMR.[5, 6] The effects of these disease etiologies can be summarized using Carpentier's functional classifications of leaflet performance.[3] Type I classification refers to MR with normal leaflet motion, and is seen with leaflet perforations or annular dilatation. Type II refers to excess leaflet motion or prolapse and occurs in the presence of chordal/PM rupture or elongation (DMR). Finally, type III function refers to restricted leaflet opening and/or closing, and is often seen in the presence of excess LV remodeling and disease (FMR). Regardless of the underlying etiology, MR may result in pulmonary hypertension, dyspnea, and atrial dysfunction, among other complications.[5]

2.2 Treatment of MR

To treat symptomatic MR, the MV structures are either repaired, or the MV is replaced altogether. As a result of the complexity of the mitral valve (Figure 2-1), many novel repair techniques have been developed. These techniques include annuloplasty, chordal replacements, papillary muscle shortening or adjustments, leaflet resections, among many other options.[7]

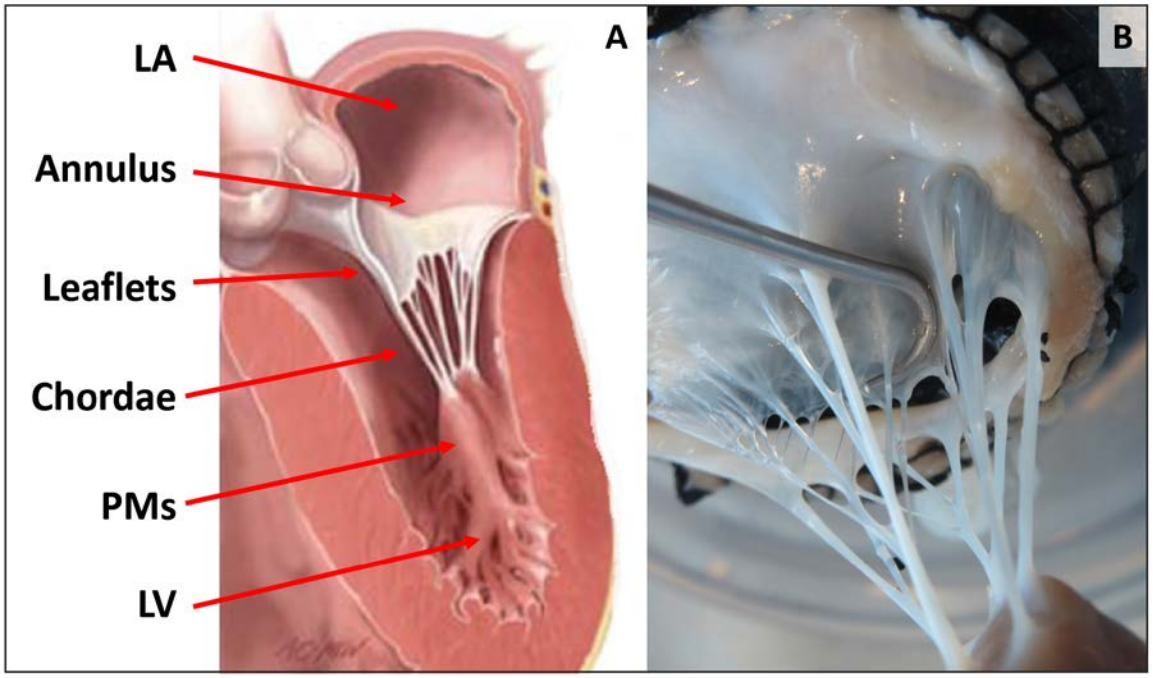

Figure 2-1 – Components and complexity of the mitral valve (MV). A schematic of the MV with labelled components is shown in (A) (Modified from Carpentier et al.[3]) An ovine MV is pictured in (B), where the true complexity of the MV can be appreciated.

Due to low perioperative mortality, and excellent long-term survival rates, surgical repair is the gold standard for DMR, and is an effective option for treating FMR.[8-10] In FMR patients, a restrictive annuloplasty is often used to down-size the dilated annulus and bring the leaflets back into coaptation. However, recurrence of MR following restrictive annuloplasty is a persistent clinical problem.[4] Studies of these patients have shown that LV sphericity, continued PM displacement and leaflet tethering are strong predictors of MR recurrence.[4, 11] These studies illustrate the importance of MV subvalvular apparatus geometry to leaflet function and repair durability.

Directly targeting the mitral leaflets, the Alfieri stitch, or edge-to-edge (E2E) repair is a surgical technique for treatment of MR (Figure 2-2A). Introduced in the early 1990's by Alfieri and colleagues[12], the E2E repair involves approximating the leaflet edges at the site of regurgitation, creating a double orifice in the mitral position. Because the E2E repair does not address ventricular remodeling, it was originally intended for DMR patients, and was often accompanied with annuloplasty for repair stabilization.[12, 13] Indeed, the E2E repair was useful only in certain situations, and often in combination with other repairs. Until recently, it was marketed as another useful "addition to the surgical armamentarium in mitral valve reconstruction."[13, 14] Regardless of the repair tool(s) used, invasive, open-heart surgery with cardiopulmonary bypass was traditionally a requirement.

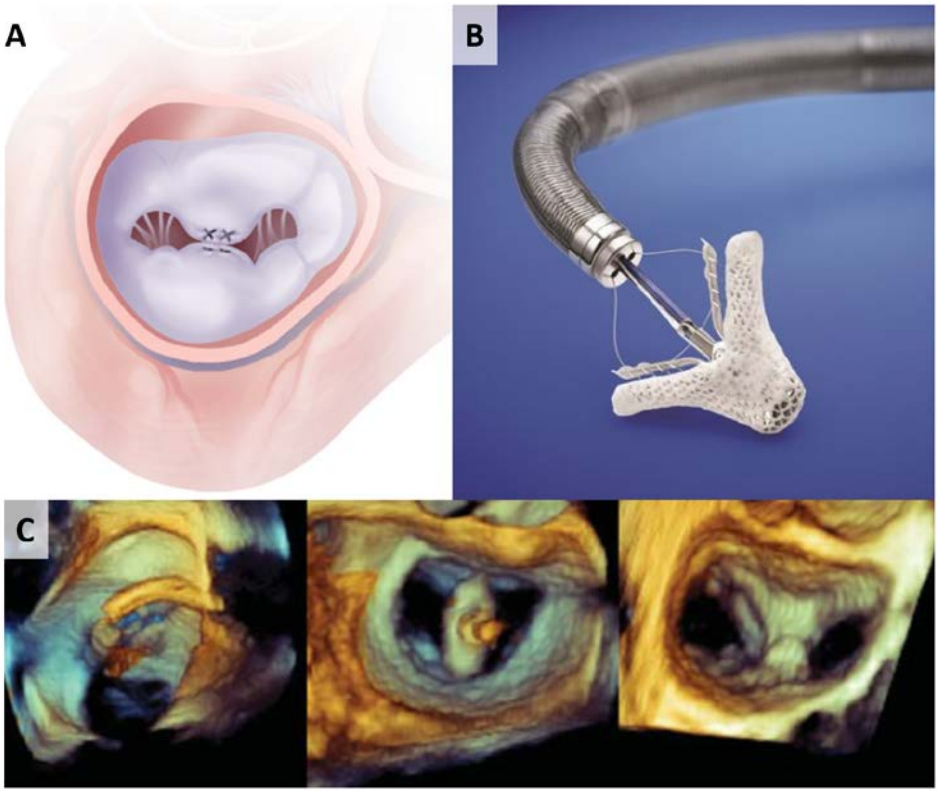

Figure 2-2 – The Alfieri stitch and MitraClip. The original edge-to-edge surgical repair technique, known as the Alfieri stitch is shown in (A) (modified from Feldman et al[15] and Rogers et al[16]). A device known as MitraClip was designed to replicate the repair percutaneously (B). Under echo guidance, the device is deployed on the beating heart as shown in (C).

2.3 Advent of MitraClip and Transcatheter Mitral Valve Repair

Many patients with MR in the older population subgroups have co-morbidities and are considered high risk for open heart surgery. In a recent study, among patients with severe symptomatic MR, a decision not to operate was made for 49% of the patients.[17] The percentage increases significantly in older populations, and in patients with low left ventricular ejection fraction, meaning that a large population of individuals with MR are simply untreatable.[17] The need for solutions to treat these high-risk patients has inspired a host of new minimally invasive endovascular repair devices.[7] In the early 2000's, a catheter-based device known as the Evalve was designed to replicate the E2E repair

without invasive and risky open heart surgery, thereby opening up a new population of patients for MR treatment.[18] This device is now known as MitraClip (Abbott Vascular, Santa Clara, CA), and is currently the only widely-used and FDA approved transcatheter mitral repair device (Figure 2-2B).

MitraClip is an MRI compatible, catheter-delivered cobalt-chromium device. Two grippers grasp and approximate the edges of the anterior and posterior mitral leaflets, creating the double-orifice characteristic of the E2E repair. Using both TEE and biplane fluoroscopy for navigation, the device is positioned inside the left atrium of the beating heart directly above the target clip location (Figure 2-2C).[19] It is then advanced through the valve into the LV, and the grippers are opened fully. The MitraClip grippers are then steadily closed as the device is pulled back toward valve, in order to grasp both leaflets. Closing the MitraClip system further approximates the mitral leaflets and seals the regurgitant orifice. After delivery of the device, the operator will evaluate the resulting MR levels according to clinical guidelines.[20] Per those guidelines, if MR reduction to ≤2+ is not achieved following initial clip implantation, an additional clip may be implanted.

2.4 Indicated and Off-Label MitraClip Usage

MitraClip indications for use (IFU) denote a narrow range of patients amenable to the treatment (Figure 2-3). The IFU indicates that the device is only to be used in degenerative MR for Type I or Type II leaflet motion. Furthermore, only patients with central MR where posterior leaflet length ≥ 10 mm, mitral valve area (MVA) > 4 cm^2, coaptation depth < 11 mm and coaptation length > 2 mm are deemed amenable to MitraClip.[19, 21] However, because the device has very low rates of adverse events, and is still the only treatment

option for many patients, it is being widely used in Europe, and off-label in the US, to treat FMR with varying degrees of success.[16, 21-23] Additionally, as many as four devices have been implanted in a single patient in Europe.[24] It is clear that the device is now being creatively used to treat a multitude of more complex leaflet functions and anatomies, but the two of the biggest limitations appear to be MitraClip detachment, and undesired development of mitral stenosis (MS),[25] or blockage of forward flow through the mitral valve.[16]

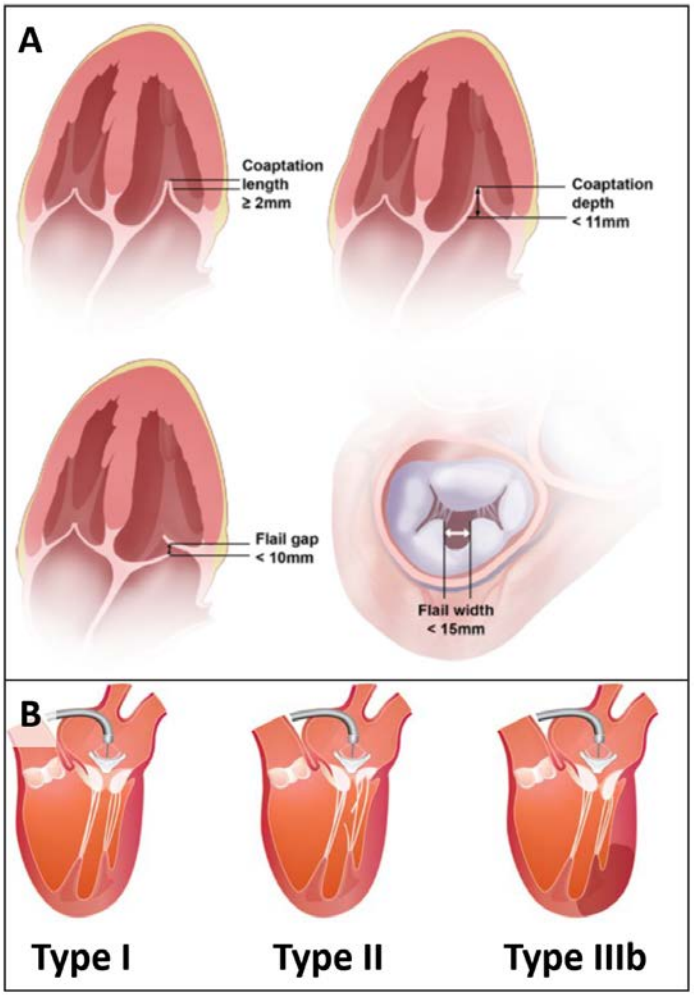

Figure 2-3 – Patient characteristics amenable to MitraClip. Coaptation and regurgitant orifice geometries from the IFU are shown in (A) and leaflet function types are shown in (B). (modified from Feldman et al[15] and Rogers et al[16])

2.5 Engineering Analysis of MitraClip and Edge-to-Edge Repair Function

Since its inception, numerous *in vitro* and *in silico* analyses of MitraClip and E2E repair have been conducted to understand both the biomechanical impact of the repair on the leaflet tissue, and the hemodynamic impact on flow through the MV in diastole.[26] First, *in vitro* left heart simulators have been applied to study the force imparted to the E2E repair across the cardiac cycle,[27, 28] as well as the effectiveness of E2E repair in the setting of displaced PMs (Figure 2-4A).[29] These studies have shown that force on the repair is generally larger in systole, and larger in the setting of annular dilatation.[27, 28] Repair effectiveness in reducing MR was generally worse in the setting of FMR with annular dilation and PM displacement.[29, 30] Similar *in vivo* investigations have corroborated a greater force on the repair with annular dilatation, but have found peak force to occur in peak diastole, which could be caused by dynamic annular dilatation.[31, 32] These findings can be applied to understand the mechanics of MitraClip detachment and/or tissue stress. However, the studies were performed only on single central repair placement, and generally in larger MV samples, where creation of MS was highly unlikely. In a recent study by Sturla and colleagues, MitraClip was implanted in *ex vivo* porcine hearts, and mean diastolic MV gradient (MVG) was measured as a function of heart rate to quantify MS.[33] Mean MVG was found to increase as a function of heart rate, however, due to the size of the porcine MV samples, no significant MS was observed.

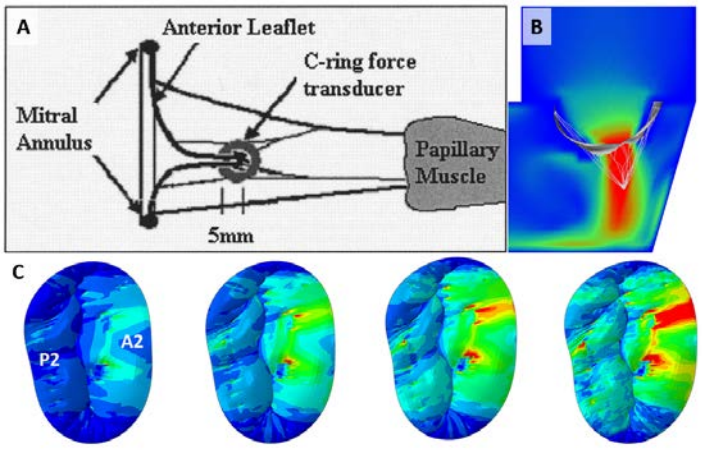

Figure 2-4 – Computational and *in vitro* analysis of edge-to-edge (E2E) repair and MitraClip. Force transducers have been used to study the loading imparted to the E2E repair by the leaflets *in vitro* (A). Fluid structure interactive models have been used to assess fluid flow through the MV after E2E repair (B). Finally, stress and strain in the mitral leaflets has been measured following full and partial MitraClip grasping (C). Modified from (A) Jimenez et al[28], (B) Lau et al[34], and (C) Sturla et al.[33]

Computational models have been applied to further understand the stress in the MV leaflets following E2E repair (Figure 2-4B,C). Starting in the late 1990's, Kunzelman and colleagues performed structural analysis on idealized MV geometries, simulating MV closure, PM displacement, annuloplasty, and chordal replacement techniques.[35-37] Shortly thereafter, Alfieri, Maisano, Votta and colleagues used structural computational modeling to simulate the E2E repair technique and investigate stress in the MV under conditions of annular dilatation, systolic pressure, and diastolic pressure.[38, 39] These structural studies show that the stress on the MV leaflets is related to the dilatation of the MV annulus, and that two distinct loading peaks are imparted on the leaflets: one at peak systole, and one at peak diastole.[38] More recently, fluid-structure interactive models have been applied to understand the flow of fluid through the MV in diastole, when E2E repair is simulated (Figure 2-4B). Lau and colleagues have shown an increase in mitral inflow velocity and a reduction in MVA after central E2E repair simulation.[34]

2.6 Treating Mitral Regurgitation Without Causing Mitral Stenosis

The central focus of benchtop and computational models has been the leaflet force on the E2E repair and MitraClip, and the stress in the leaflets. However, the elevation of MVG and reduction of MVA leading to the undesired creation of MS is a clinically acknowledged risk in certain cases.[16, 25, 40, 41] A recently published report by Neuss et al has shown that significantly poorer long-term patient outcomes result when a patient is left with a mean MVG above 5 mmHg after MitraClip implantation.[40, 42] On the other hand, reduction of MR to <2+ is also critical to achieve optimal patient outcomes.[43] Additional clips may be deployed to reach this level of MR reduction, but the benefits of MR reduction and concomitant risk of increased MS severity with each clip must be balanced.[40] In general, additional clips are not placed if mean MVG is found to be ≥ 4 mmHg.[44] Relevant thresholds for MS severity[45], along with the threshold for placing additional clips are summarized in Table 2-1.

Table 2-1 – Mitral Stenosis (MS) cutoff values. Mild, moderate and severe values from guidelines, and cutoff values for additional clip placement from clinical experience are shown. MVA – MV area; MVG – MV gradient

Level	MVA (cm^2)	Mean MVG (mmHg)
Cutoff: Place another Clip?	>2.5	<4
Mild MS	>1.5	<5
Moderate MS	1.0-1.5	5-10
Severe MS	<1.0	>10

Though undesirable creation of MS may be a consequence of MitraClip therapy, well established guidelines and practices are currently in-place to avoid such a result.[40, 44] For example, as per the MitraClip IFU and pivotal US clinical trials (EVEREST I,II), MR patients with baseline MVA<4.0 cm^2 are contraindicated for MitraClip treatment.[15] Further supporting this, Herrmann and colleagues have confirmed that MitraClip repair in patients with a baseline MVA above this cutoff did not result in significant MS when implanting up to two devices.[46]

2.7 Challenges of Treating Functional Mitral Regurgitation with MitraClip

It is important to note that the above guidelines are well established in patients with DMR.[19] Contrary to DMR, MitraClip is currently not approved in the US for treatment of FMR. In FMR, severe dilatation of the LV and PM displacement can cause diastolic restriction (Type III) of the anterior mitral leaflet (AML), complicating use of leaflet based interventions such as MitraClip.[47] A recent study by Chan *et al* illustrates that use of MitraClip in the setting of AML tethering can cause elevated mean MVG under certain conditions. The authors report that there is often a "compromise" between complete elimination of MR and significant increase in mean MVG due to placement of additional clips, and the planned clip strategy must be aborted.[48] This compromise was most often observed in patients with FMR, rather than DMR. Furthermore, in this small group of 12 patients with FMR, the authors found that compromise occurred most often in those patients with more AML tethering.

It is clear that baseline MVA and number of clips implanted can affect the likelihood of inducing MS. Additionally, leaflet tethering commonly seen in FMR appears

to be an important factor affecting resultant MS severity, but our understanding of the effects of MitraClip in the setting of AML tethering is still incomplete. A quantitative description of the impact of baseline MVA, MitraClip placement, *and* severity of AML tethering on resulting MS severity would provide useful information toward patient selection for treatment with transcatheter edge-to-edge MV repair devices such as MitraClip.

CHAPTER 3: HYPOTHESIS AND SPECIFIC AIMS

MitraClip (Abbott Vascular, Santa Clara, California) is currently not approved in the US for treatment of functional mitral regurgitation (FMR), but is widely used off-label for this purpose. In many cases, multiple MitraClip devices are used to treat MR[43] though placement of additional devices can further reduce mitral valve area (MVA) and increase of mean mitral valve gradient (MVG), leading to mitral stenosis (MS).[45] In FMR in particular, MS severity after MitraClip may be further exacerbated by diastolic restriction of the anterior mitral leaflet (AML) caused by severe dilatation of the left ventricle (LV) and papillary muscle (PM) displacement [48]. However, limited data on the effect of AML tethering on MVA and MVG after MitraClip exists. The central hypothesis of this study is that **obstruction of flow through the mitral valve will be exacerbated by both MitraClip placement *and* by restriction of the AML during diastole, and that a greater incidence of MS will be observed when both factors are present than with either alone**. This could provide useful information toward patient selection for treatment with transcatheter edge-to-edge MV repair devices.

Specific Aim 1: Develop a left heart simulator capable of repeatable, precise diastolic AML tethering, and a custom edge-to-edge clip device (GTclip) for use in SA2. To directly test the hypothesis, methods of repeatably controlling and measuring AML tethering on excised ovine MV samples must first be developed. Secondly, a custom edge-to-edge clip (GTclip) will be developed. This device will model the bite dimensions and profile of the MitraClip device, allowing MitraClip implantation to be simulated.

Specific Aim 2: Use the tools developed in SA1 to assess MV forward flow obstruction as a function of baseline MV annular area, AML tethering severity, and positioning of GTclip devices. The severity of MS is expected to vary as a factor of MV annular area, AML tethering severity, and placement of GTclips. On each MV sample, placement of one or two GTclips will be performed in common locations. AML tether severity will be varied among three levels for each GTclip placement. Baseline mitral annular area will be varied from sample to sample. Quantification of MS severity as a function of these factors will yield useful information toward patient selection for treatment with transcatheter edge-to-edge MV repair devices.

CHAPTER 4: MATERIALS AND METHODS

4.1 Left Heart Simulation Platform

4.1.1 Left Heart Simulator Components and Operation

The GT Left Heart Simulator (GTLHS) (Figure 4-1) consists of a clear acrylic left atrium and ventricle. A pulsatile piston pump (Vivitro Labs, Inc. Victoria, BC, Canada) drove flow through the system, and systemic resistance/compliance elements were manually adjusted to achieve physiological pressures and flow over the cardiac cycle (heart rate – 70 beats/min, cardiac output – 5 L/min, peak LV pressure – 120 mmHg, 35% systole, 65% diastole). While typical MitraClip patients may have significantly reduced pre-procedural cardiac output (CO) due to regurgitant fractions as high as 50%, their post-procedural CO is regularly found to be in the range of 5 L/min. Therefore, the mitral inflow volume was held constant at 70 mL (5 L/min). Wall-tapped pressure transducers (Utah Medical, Midvale, UT, USA) were used to record pressure in the left atrium and ventricle, while an electromagnetic flow probe (Carolina Medical, East Bend, NC, USA) was used to record instantaneous flow rate. A Philips iE33 xMatrix quantitative echo system and X7-2 transducer (Philips Healthcare, Andover, MA, USA) were used to acquire 3D gated echo images and measure MVA.

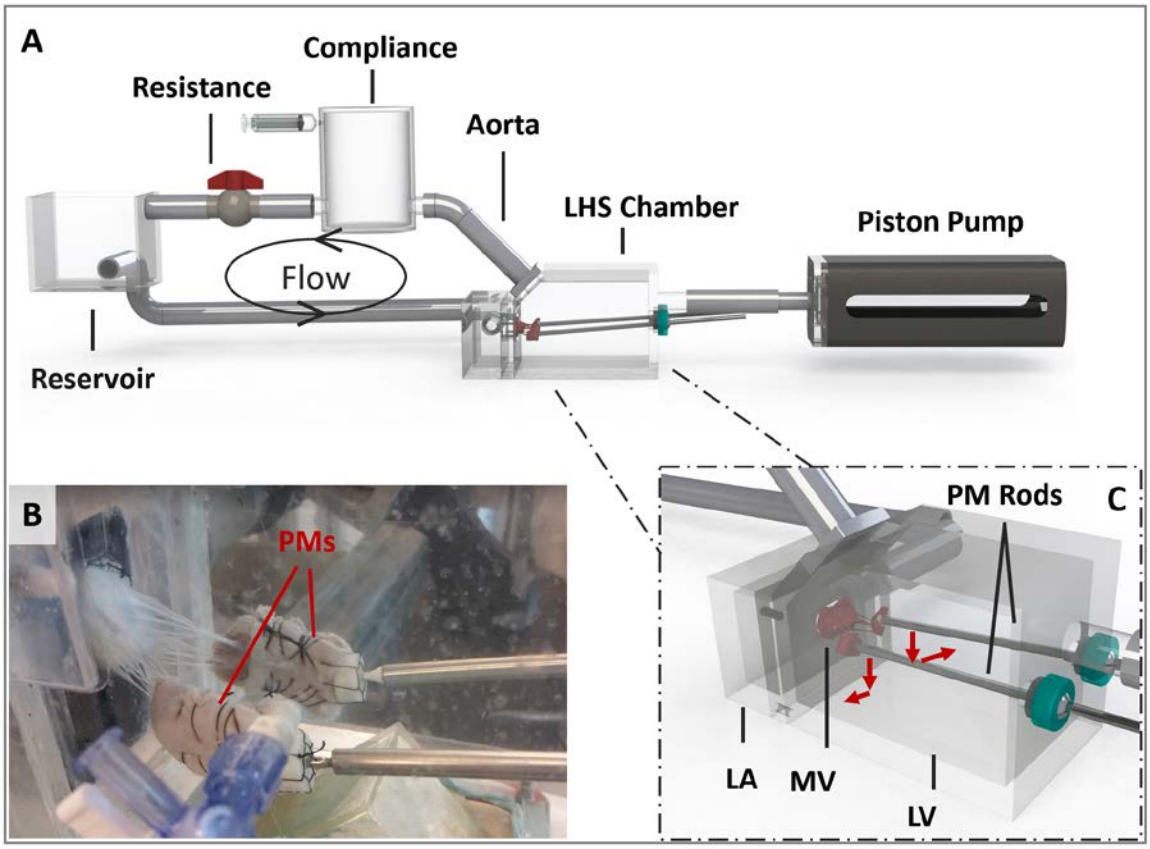

Figure 4-1 – Georgia Tech Left Heart Simulator (GTLHS) platform. The complete GTLHS pulse-duplicator is shown in (A), where a piston pump drives flow, opening and closing the MV physiologically. The excised and mounted ovine MV is shown in (B), where the papillary muscles (PMs) are tethered. GTLHS chamber components are illustrated in (C) where the symmetric PM displacement vectors used to create anterior mitral leaflet (AML) tethering are shown in red. The left atrium and ventricle (LA and LV) of the GTLHS are also denoted.

4.1.2 Papillary Muscle Rod Control

Papillary muscles (PMs) were affixed to 1/4" stainless-steel rods for positional control and anterior leaflet tethering. The rods were mounted through ball-in-socket joints on the apical plate of the GTLHS (Figure 4-1). The PM position was controlled in three dimensions by manually manipulating the PM rods on the exterior of the GTLHS.

4.1.3 Adjustable Annulus Design and Construction

A custom adjustable annulus plate was constructed to control the baseline mitral annular area (MAA) for MV samples (Figure 4-3). As opposed to MAA, MVA is the area of the MV at its most narrow point, and is typically used to assess suitability of patients for MitraClip. With normal diastolic leaflet function, MAA and MVA may be comparable, however, Kubota and colleagues have shown that severe leaflet tethering may significantly reduce MVA.[49] The range of MAA values used in this study was 3.6 to 4.8 cm^2, in order to account for the effect of leaflet tethering on MVA reduction. This was intended to create baseline MVA values of 4.0±0.5 cm^2. This range was targeted, because patients with baseline MVA just above or below the minimum MVA of 4.0cm^2 may be more prone to MS following MitraClip than patients with higher baseline MVA.[46] Nevertheless, patients with baseline MVA in this range are commonly treated with the device in a real-world setting.[46, 48]

The custom adjustable annulus plate was designed and assembled as follows. A 5.0 cm^2 annular profile was first laser-cut from an elastic neoprene skirt, and from a rigid PETG plastic sheet (McMaster-Carr part no. 1580T3 and 9513K82, respectively). The elastic neoprene skirt was then sutured to the perimeter of the plastic sheet (Figure 4-2). Next, a stainless-steel wire was imbedded in the suture cuff surrounding the annulus using a Ford interlocking stitch, such that tension applied to the wire constricted the annulus to as small as 3.6 cm^2.

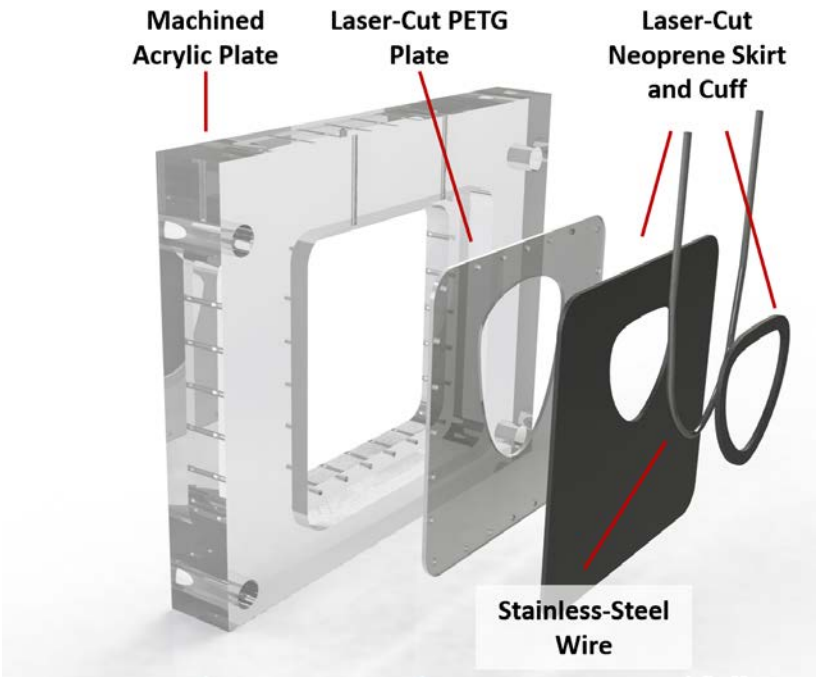

Figure 4-2 – Adjustable annulus plate design and assembly. The base of the plate (left) is machined from acrylic, and interfaces with the left atrial and ventricular chambers of the Georgia Tech Left Heart Simulator (GTLHS). A laser-cut polyethylene terephthalate-glycol (PETG) plate is sealed against the acrylic base, providing support for the flexible neoprene skirt, which is sutured to the PETG plate. A stainless steel wire is imbedded within the neoprene skirt and cuff.

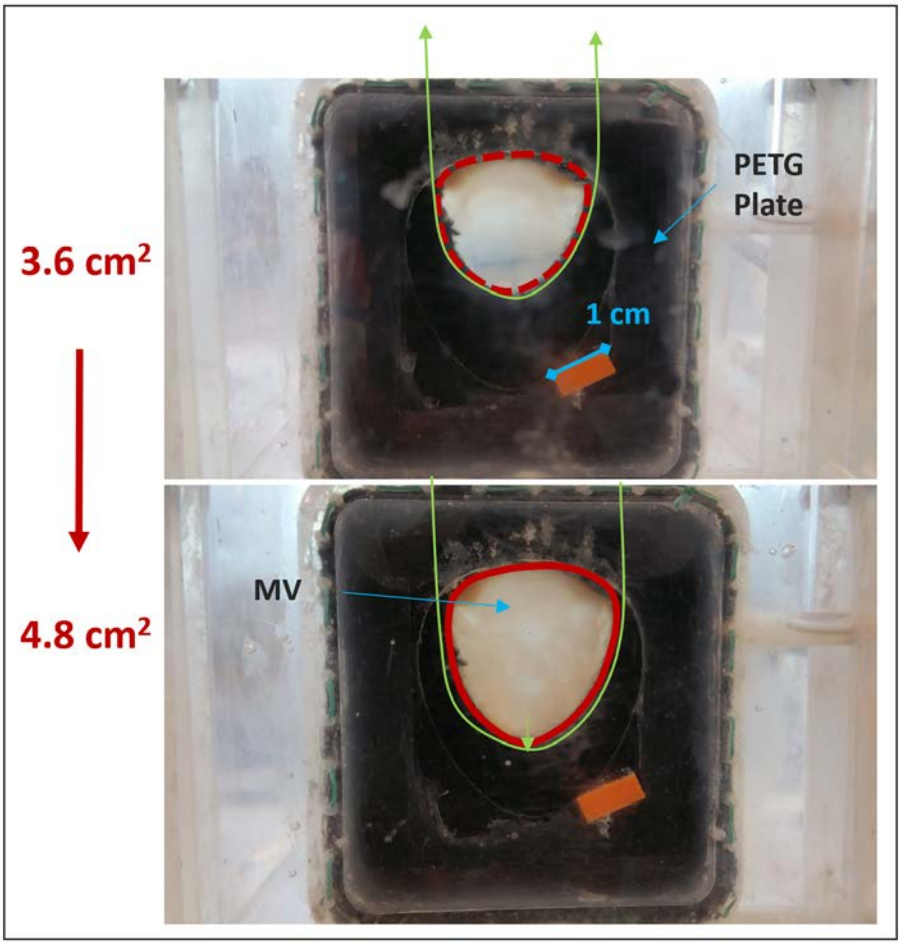

Figure 4-3 – Adjustable annulus plate design and function. An *en face* view of the MV from the atrium shows the operation of the adjustable annulus plate. Applying tension to a stainless-steel wire (green line) embedded in the annulus allows for adjustment of the annular size. A 1 cm calibration strip on the plate allows for measurement of the annular size on digital images (red annular outlines).

A rigid acrylic plate was cut to fit between the atrium and ventricle of the GTLHS chamber. A pocket was machined into the plate such that the adjustable annulus assembly could be mounted within the rigid plate and vertical holes were drilled through the acrylic plate at the trigones. Finally, the stainless-steel wires were fed through those vertical holes, and the adjustable annulus assembly was sealed to the acrylic plate with silicone, completing assembly of the adjustable annulus. A 1 cm length plastic strip was affixed to the assembly on the atrial side just below the annulus. By taking an *en face* digital image

of the annulus and calibrating pixel length to the 1 cm strip, the MAA could be precisely measured on the digital images (Figure 4-3, APPENDIX B.1).

4.1.4 Mitral Valve Selection and Preparation

Ovine hearts of approximately 1 lb in total weight were sourced from an abattoir (Superior Farms, Dixon, CA, USA). The left atrium was trimmed from the heart, allowing visualization of the MV. A size 26 Edwards Physio annuloplasty ring sizer was used to confirm that the inter-trigonal distance of the MV sample matched the geometry of the annulus plate. After confirmation, an incision was made through the aorta and through the anterior aspect of the LV, between the PMs. Care was taken to preserve the chordae and PMs as the LV was cut open. Next, a medial cut was made to separate the right heart, and the excess tissue on the apex of the heart was removed. Two cuts were then made to separate the PMs from the annulus, then from each-other. The annular myocardium was then trimmed, leaving ~3-5 mm of myocardium above the color-change line of the annular hinge (Figure 4-4).

Next, the annulus was sutured to the adjustable annulus plate. An initial single mattress suture was placed at the center of the anterior annulus, and matched to this location on the annulus plate. Three more mattress sutures were then placed at each trigone and at the center of the posterior annulus in the same way. Finally, a Ford interlocking stitch was started at the right trigone, and, placing each stitch 2-4 mm apart following the entire annular circumference, the annulus was sutured to the plate (Figure 4-4).

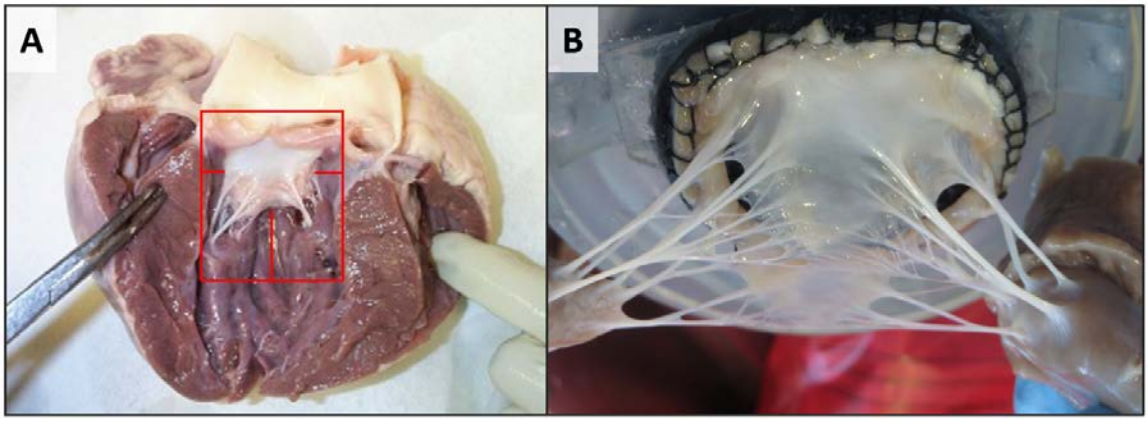

Figure 4-4 – MV excision and mounting. An incision is first made through the aorta and the anterior wall of the LV, revealing the MV (A). Cuts are then made along the red lines to separate the myocardium, atrium and right ventricle from the MV, separate the PMs from the annulus, and separate the PMs from each other (A). Care is taken to preserve the leaflets, chordae, annulus and PMs. The annulus is sutured to the annulus plate of the GTLHS using a ford interlocking stitch (B).

Cotton jersey knit (T-Shirt) fabric was used to create pouches encapsulating the PMs. A square of fabric was cut out and sized to the PM size. The fabric was wrapped around the PM long-ways from the chordal insertions to the back of the PM, leaving the sides open. Two running sutures starting from the base of the PM near the chordae were used suture the fabric together at either side of the PM (Figure 4-5). Further information on MV excision, MV mounting, and GTLHS setup and operation can be found in previous publications[50-52] as well as protocols listed in the catalogue of data storage in APPENDIX C.

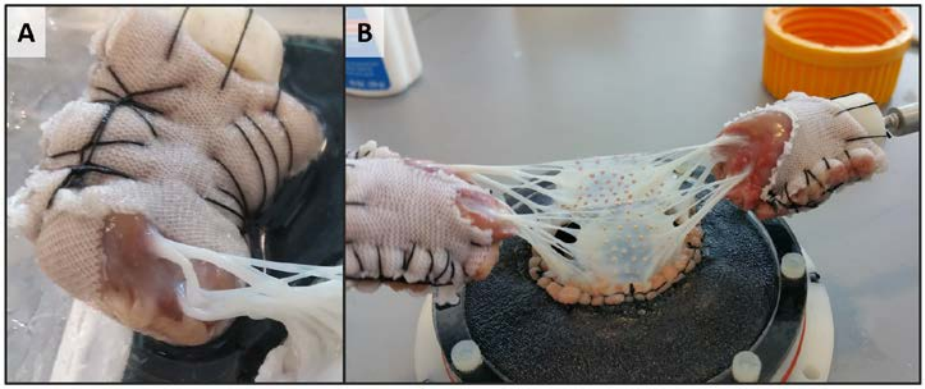

Figure 4-5 – Papillary muscle (PM) preparation. Cotton jersey knit (T-Shirt) fabric was used to create pouched encapsulating the PMs (A). After folding a rectangular section of the fabric long ways over the PM, two ford interlocking-stitches running up either side of the PM secures the fabric to the PM. Next, the plastic PM attachment is sutured to the PM. The fully mounted and prepped MV is shown in (B).

4.2 Anterior Leaflet Tethering

4.2.1 Papillary Muscle Displacement

In FMR, LV dilatation causes PM displacement.[4] This can cause leaflet tethering at a range of severities.[47] This range was targeted for this study, in order to understand the effect of simulated MitraClip on forward flow obstruction in the setting of varying degrees of leaflet tethering, ranging from mild to severe. To achieve this effect *in* vitro, PMs were displaced laterally and posteriorly by adjusting the PM control rods on the exterior of the GTLHS, tethering the anterior mitral leaflet (AML) at three levels. AML tethering severity was assessed by the angle of the AML with respect to the annular plane, and is referred to as AML tether angle. The GTLHS adjustable annulus plate featured a planar annulus, allowing non-ambiguous definition of the annular plane and AML tether angle. AML tether angles of 75° (mild), 60° (moderate), and severe (45°) were replicated in this experiment. These levels were based on published human data quantifying AML tethering severity in FMR patients (Figure 4-6).[47]

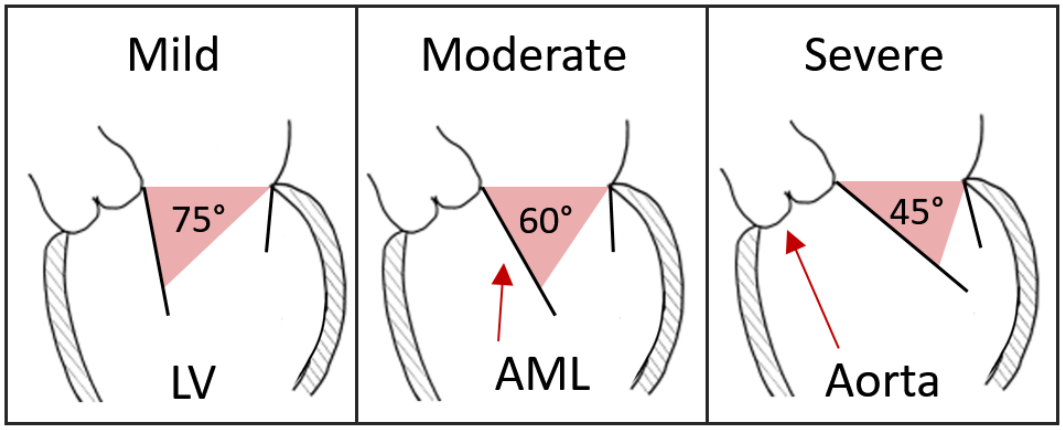

Figure 4-6 – Mild, moderate and severe anterior mitral leaflet (AML) tether angle. AML tether angle was defined as the excursion angle of the AML from the mitral annular plane. (AML tethering diagrams modified from Otsuji et al[47])

4.2.2 Anterior Leaflet Angle Measurement

PMs were displaced laterally and posteriorly in a symmetric manner, and AML tether angle was measured using 3D echo. PM displacement was empirically adjusted until reaching each target angle, as confirmed by 3D echo. Using the Philips 3DQ Measurement tools, a plane was positioned to bisect the MV on the A2/P2 plane (mid-point of the anterior/posterior leaflet) in peak diastole. Next the distance measurement tool was used to measure the three sides of a triangle, with the sides corresponding to the annular width, AML length and span from the anterior leaflet tip to the posterior annulus. The angle between the annular plane and the AML, θ, was calculated using Equation 1, where L_{AML} is the length of the AML, L_{Ann} is the distance from A2 to P2, and L_{Span} is the distance from the AML tip to the P2 position on the annulus (

Figure 4-7).

$$\theta = \cos^{-1}\left(\frac{L_{Span}^2 - L_{AML}^2 - L_{Ann}^2}{-2(L_{AML}^2 * L_{Ann}^2)}\right) \quad (1)$$

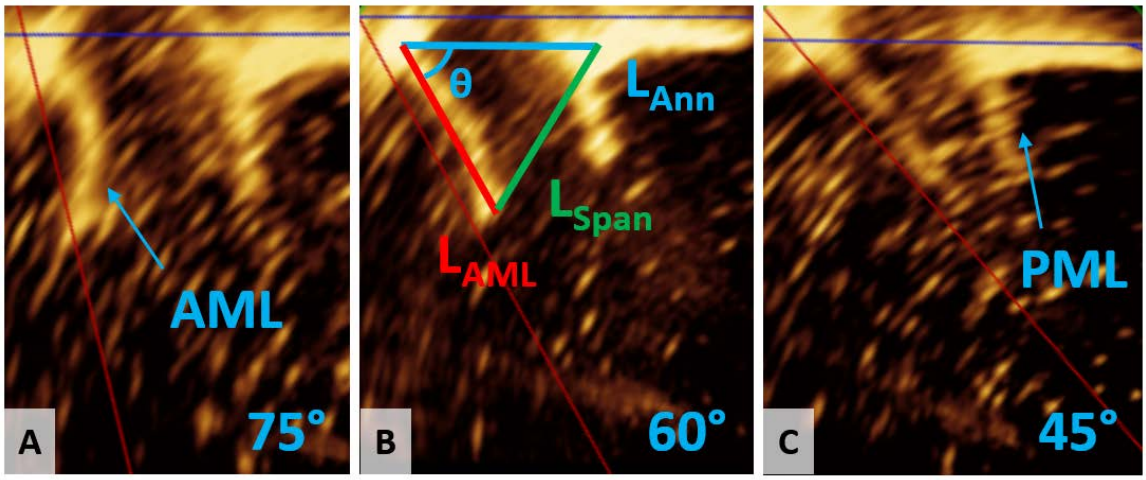

Figure 4-7 – Measurement of AML tether angle using 3D echocardiography. For each anterior mitral leaflet (AML) tether angle, the distance from the annulus to the AML leaflet tip, L_{AML}, was measured, followed by the width of the annulus, L_{Ann}, and the span between the posterior annulus and the AML leaflet tip, L_{Span}. The angle of the AML with respect to the annular plane was then calculated using Equation 1. PML – Posterior mitral leaflet.

4.2.3 Anterior Leaflet Angle Repeatability and Accuracy

Once a target angle was reached, location of the PM rods on the exterior of the GTLHS was recorded. The recorded markings were used to precisely re-create the AML tether angles in the second phase of each experiment, where MitraClip placement was simulated with custom edge-to-edge clips (described in section 4.3). Additionally, to secure the PMs in their specific locations corresponding to each AML tether angle, cable ties were secured around the PM rods on the exterior of the GTLHS for each target angle, pulling the PM rods medially and hoisting them anteriorly (Figure 4-8). Different cable tie loops were made for each target angle, and could be easily swapped in and out. These were used,

in addition to the markings, to precisely re-create the desired target AML tether angles when MitraClip was simulated.

To test the precision of PM positioning, a feasibility study was done on a single MV sample. PM positions were first determined for the target angles, and the PM positions were recorded for each AML tether angle. Next, the positioning methods described above were used to cycle through the progression of mild (75°), moderate (60°) and severe (45°) AML tether angles five times. For each angle and each cycle iteration, the AML tether angle was measured with 3D echo, allowing the precision and accuracy of the method to be quantified over a simulated experiment.

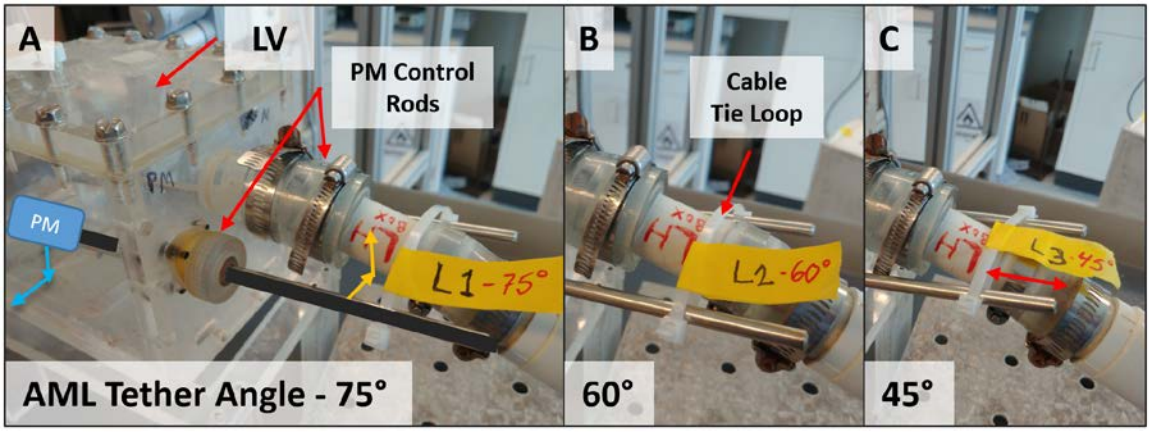

Figure 4-8 – Papillary muscle (PM) tethering method. PMs were displaced posteriorly and laterally to create anterior mitral leaflet (AML) tethering (blue arrows, A). PM control rods on the exterior of the GT left heart simulator (GTLHS) were pulled medially and hoisted anteriorly (yellow arrows, A). Cable tie loops were secured to the PM control rods on the exterior of the GTLHS to affix the PMs in their displaced positions (B). These cable tie loops could be swapped easily, to re-create the different AML tether angles (red arrow, C). LV – Left Ventricle

4.3 Custom GT Edge-to-Edge Clip Design, Fabrication and Use

4.3.1 Design Constraints and Functions

Prototype Georgia Tech edge-to-edge clips (GTclips) were designed to replicate the bite profile and dimensions of the MitraClip device (Figure 4-9). The MitraClip bite profile was obtained from the MitraClip IFU and is approximately 5 mm wide and 9 mm in length, with an overall device length of approximately 15 mm. The GTclips were machined from tough polycarbonate plastic and stainless steel. A cross-hatch pattern was etched into the gripping face of the clip to prevent clip detachment.

4.3.2 Concept and Engineering Drawings

These GTclips functioned in a similar manner to alligator clips, which allowed them to be quickly deployed and re-positioned without damaging the leaflets (Figure 4-9B).

4.3.3 Materials Selection

Due to the small size of features in the GTclip design, polycarbonate (PC) was selected for its high IZOD impact strength, and high elongation at break. Acrylic is another plastic commonly used in CFM lab applications, but small features tend to crack and fracture easily when fabricated from acrylic. The low specific gravity of PC compared to metals and steels is also desirable, to bring the GTclip close to neutral buoyancy. The spring elements at the back of the GTclip were made from 0.008” thick spring-tempered 301 stainless steel strip sourced from McMaster-Carr (part no. 2416K42). The spring-temper is critical, so that the spring element does not plastically deform when opening the clip, and fail to provide closing force to the clip.

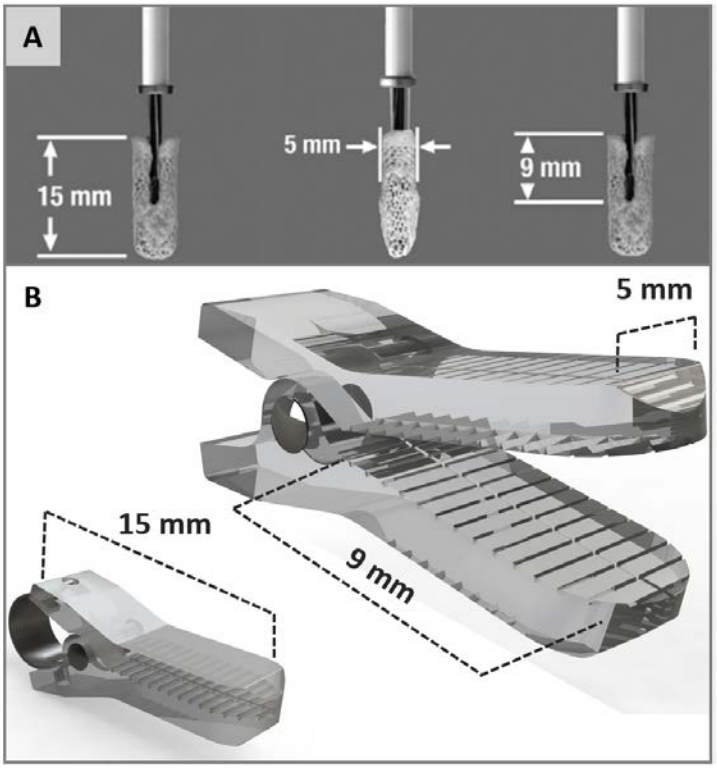

Figure 4-9 – Custom edge-to-edge (GTclip) design. Device dimensions from the MitraClip IFU are shown in (A). Dimensions and computer aided design (CAD) of the GTclip are shown in (B).

4.3.4 Fabrication and Assembly

The PC grippers were CNC machined from a single PC sheet. The CNC tool paths were generated with HSMworks in SolidWorks (Dassault Systemes, Waltham, MA, USA) (Figure 4-10A,B). Engineering drawings are shown in APPENDIX B.2. Following machining, the parts were de-burred and a gripping pattern was cut into the gripping face of the parts by hand using a razor blade (Figure 4-10C,D). Next, a stainless-steel pin was placed in the actuating joint to hold two grippers together. A 2-0 black silk suture was used to tie the two grippers together. Finally, a rotary tool was used to cut out the spring steel elements. These were bent into shape using needle nose pliers and secured between the two grippers at the back of the GTclip (Figure 4-10E,F).

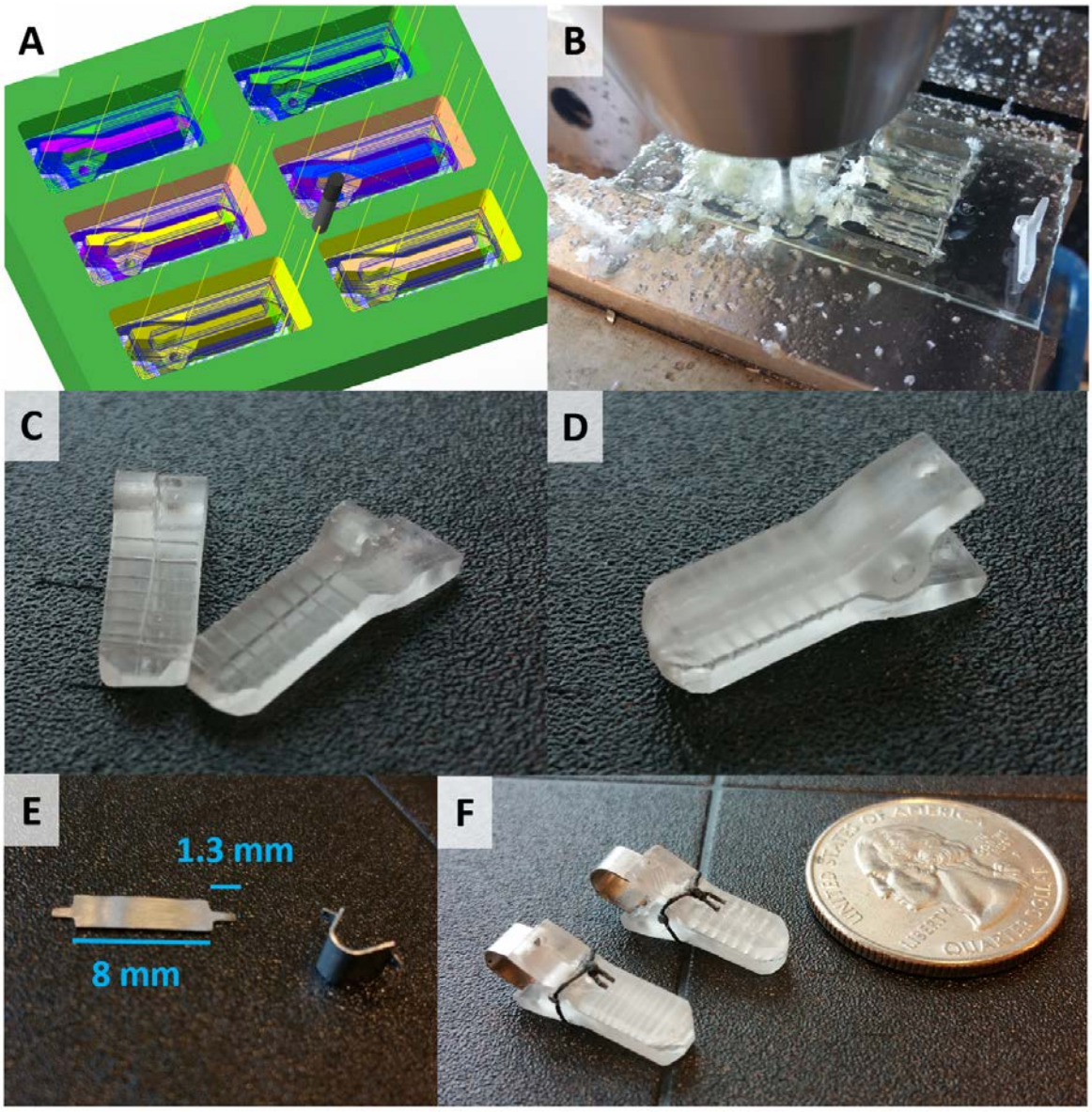

Figure 4-10 – Custom edge-to-edge clip (GTclip) fabrication and assembly. Tool paths for CNC machining were designed in HSMworks for SolidWorks, and the GTclip grippers were machined from a single sheet of polycarbonate (A,B). The grippers were de-burred and a gripping pattern was cut into the gripping face with a razor blade (C,D). The spring element was cut from a spring tempered 0.008" thick 301 stainless steel strip using a rotary tool. The spring element is dimensioned as shown in (E). The final assembled GTclip devices are shown in (F).

4.3.5 GTclip Implantation

GTclip was quickly and easily installed on MV samples for this experiment (Figure 4-11A). Minimal echo attenuation and noise was observed from the mostly-plastic design (Figure 4-11 B-D). Over the course of data collection, no instances of clip detachment or leaflet damage were observed. In order to understand how placement of one or two MitraClip devices in common locations on the MV affects forward flow obstruction in the setting of AML tethering, four common implantation positions[44, 46, 53] were selected for this experiment (Figure 4-12). The single central clip placement is the standard placement of MitraClip for central MR.[15, 43] If significant MR persists following implantation of a single central clip, another clip may be deployed next to the first, creating the double central clip placement.[54] In cases of non-central MR, placement of the device in the commissure is commonly performed.[55] When MR persists, an additional clip may be deployed more centrally, creating the central and commissural clip placement.[55] These four strategies were replicated with GTclip for each MV sample in the experiment (Figure 4-12).

4.3.6 GTclip Bite Profile Verification

Following central implantation of GTclip in a feasibility trial, the geometry of the approximated AML and PML was compared to that of a MitraClip patient. The width of the bite profile for GTclip was measured with both 3D echo and with *en face* photogrammetry. This was compared to the width of the MitraClip leaflet bite profile in a clinical echo image of the MV in peak diastole.

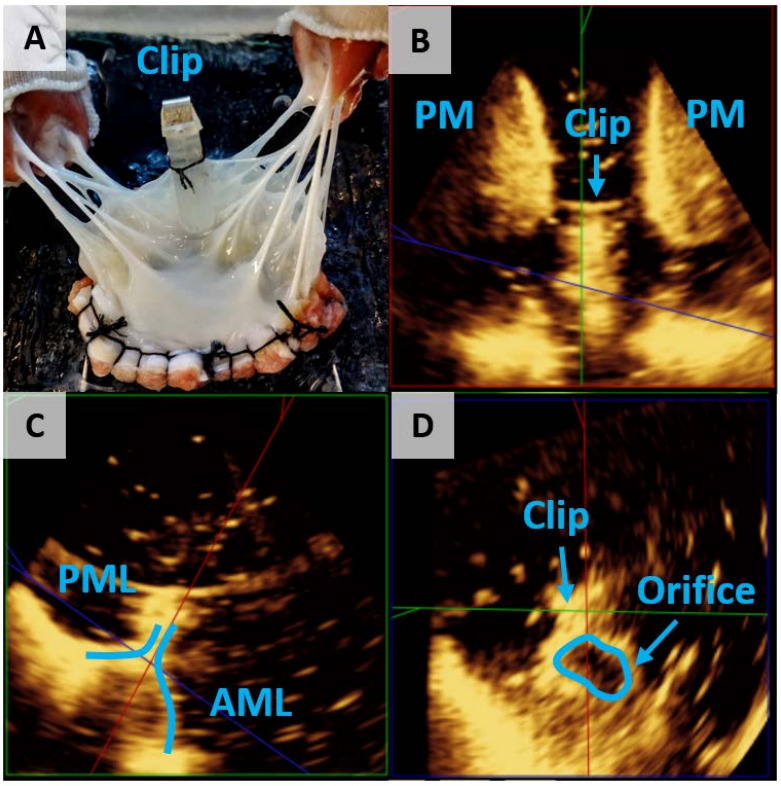

Figure 4-11 – GTclip placement. Central clip placement on an excised ovine MV sample is shown in (A). In 3D echo, the device can be seen in position (B,C). A 2D planimetry tracing of one orifice is shown (D). PM – Papillary Muscle; AML – Anterior Mitral Leaflet; PML – Posterior Mitral Leaflet.

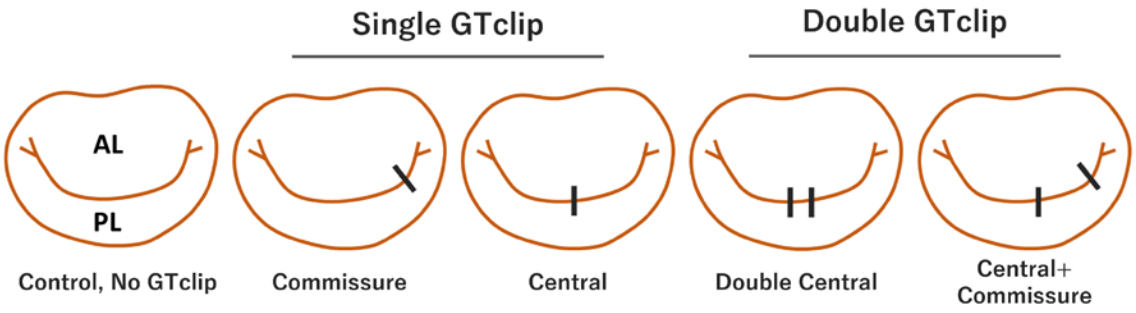

Figure 4-12 – Simulated GTclip positions. In addition to control conditions without GTclip (left), two single-GTclip placements and two double-GTclip placements were simulated. These mimic commonly used single and double MitraClip placements.

4.4 Experimental Protocol and Conditions

4.4.1 Experimental Conditions and Matrix

The experimental matrix of conditions is shown in (Table 4-1). The mitral annular area (MAA) was adjusted for each MV sample, and ranged from 3.6 to 4.8 cm^2. The MAA was not varied during the course of an experiment, but was varied between experiments. Each of the three AML tether angles was simulated before GTclip implantation, and for each of the four GTclip placements, yielding fifteen different conditions for each experiment.

4.4.2 Experimental Protocol

For each experiment, PM positions were first determined for each AL tethering angle with no clips implanted, and corresponding retainers were adjusted for each angle. Once each desired AL tether angle was reached, pressure and flow waveforms were recorded along with 3D gated echo images. Next, the commissural clip placement was simulated, and the three AL tether angles were sequentially re-created using the set of retainers. Pressure and flow waveforms, and 3D gated echo were recorded at each AL tether angle. These steps were repeated for each subsequent clip placement strategy (single central, double central, commissural/central).

Table 4-1 – Experimental matrix of conditions. Test conditions simulated on each MV sample for the experiment.

Conditions repeated for each MV sample (N=6)

Group No.	GTclip Placement	AL Tether Angle
1	None 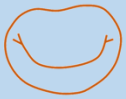	75°
2		60°
3		45°
4	Commissure 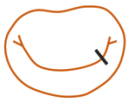	75°
5		60°
6		45°
7	Central 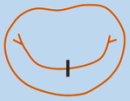	75°
8		60°
9		45°
10	Double Central 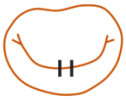	75°
11		60°
12		45°
13	Central/Commissure 	75°
14		60°
15		45°

4.5 Experimental Measurements

4.5.1 MV Pressure Gradient

Mean and peak MV gradients (MVG) were measured during the diastolic phase of the cycle using the pressure transducer recordings. The difference between instantaneous atrial and ventricular pressure was computed, then the mean of the gradient was computed for the diastolic phase of the cycle using MATLAB R2016B (MathWorks, Natick, MA, USA). The maximum magnitude of the diastolic gradient was recorded for peak MVG value. The change in mean/peak MVG from pre-clip to post-clip was also computed for each GTclip position.

4.5.2 MV Area

Peak diastolic MVA was manually measured by planimetry on the 3D Echo images using Philips QLab 9.0 3DQ software (Philips North America, Andover, MA, USA), and the change in MVA from pre-clip to post-clip was computed. MVA was measured following established echocardiographic technique[56]; an orthogonal plane was placed perpendicularly to the valve leaflets at peak diastole, and the orifice was carefully traced within the measurement plane. In the case of multiple orifices, planes were independently placed to measure each orifice, then summed for total MVA (Figure 4-11D). Measurements on each image were made three separate and independent times, and the intraclass correlation coefficient with 95% Confidence Interval (95%CI) was found to be 0.983 (0.977-0.989), indicating that measures were reliable.

4.5.3 Fluid Forces on the MV Apparatus

Ideally, the AML will impose minimal resistance to the fluid flowing from the LA to the LV in diastole. Increased resistance to forward flow due to AML tethering and GTclip placement indicates that the fluid is imparting a greater force on the MV apparatus. Estimating the change in fluid force caused by GTclip and AML tethering may shed light on the mechanics of forward flow obstruction and redirection. Here, fluid flow through a narrowing pipe bend was assumed as a simplified model of the effect of the tethered MV on the diastolic filling flow (Figure 4-13).[57]

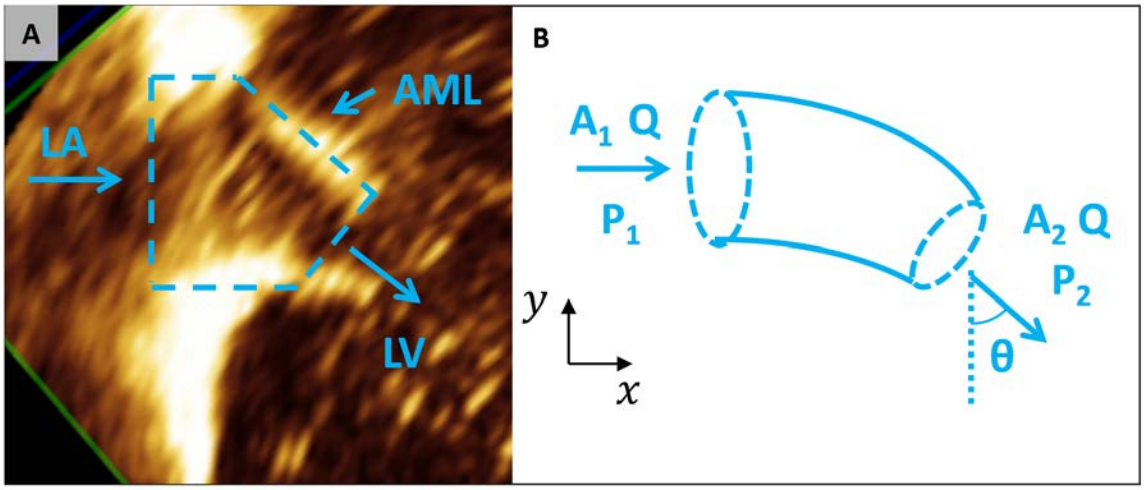

Figure 4-13 – Reaction force on the tethered anterior mitral leaflet (AML). Fluid flow through the MV in diastole can be modeled as a pipe-bend. A cross section of the MV under severe tethering is shown in (A), where the AML, left atrium (LA), and left ventricle (LV) are shown. The control volume analysis is shown in (B).

Reducing the governing equation describing conservation of momentum, reaction force of the valve on the inflow jet is described by Equations 2 and 3 below, for force in the x-direction, R_x, and in the y-direction, R_y, respectively. Here, β is the angle of the AML to the horizontal (90°-AML angle). A_1 and p_1 represent the annular area and peak diastolic atrial pressure, respectively, while A_2 and p_2 represent the peak diastolic MVA and ventricular pressure, respectively. Finally, Q is the peak instantaneous flow rate through the valve in diastole.

$$R_x = \rho Q^2 \left[\frac{1}{A_1} - \frac{1}{A_2} cos\,\beta\right] + A_1 p_1 - A_2 p_2\, cos\,\beta \tag{2}$$

$$R_y = (\rho \frac{Q^2}{A_2} + A_2 p_2) sin\,\beta \tag{3}$$

The drag force (N) of the inflow jet on the MV apparatus in the direction of the inflow jet is represented by R_x. Total fluid force (N) on the MV apparatus was determined

by calculating the magnitude of the force vector by Equations 2 and 3. These metrics were calculated for each experiment, and each condition.

4.6 Statistical Analysis and Modeling

All statistical tests and modeling was conducted using Minitab 18 statistical software (Minitab Inc, State College, PA, USA). Additionally, unless stated otherwise, all results are presented as mean ± 95% confidence interval.

4.6.1 General Linear Model: Independent Variables, Covariates, and Dependent Variables

Within the experimental model, AML tether angle and GTclip configuration were treated as independent categorical variables. The MAA for each valve was introduced as a continuous covariate variable. These make up the three independent variables controlled in this study. The dependent variables were MAA, mean MVG, peak MVG, total fluid force, and drag force. A general linear model (GLM) was fitted to the data for five separate analyses on the resulting MVA, mean MVG, peak MVG, total fluid force, and drag force. Additionally, a GLM was fitted to the post-clip increase mean and peak MVG over baseline without GTclip, and the decrease in post-clip MVA below baseline without clip. The model fit for each group is described by Equation 4,

$$y = k + (MAA)\alpha + \beta + \gamma + \varepsilon \qquad (4)$$

Error! Bookmark not defined.where y is the dependent variable, ie. estimated MVA/MVG measurement. The coefficients on the right-hand side of the equation are

statistically calculated by the minitab GLM to best fit the changes observed in the dependent variable. The first term on the right side, k, is a constant offset coefficient. The second term is adding the effect of the continuous variable, MAA, which is directly multiplied by its slope coefficient, α, to give the contribution of MAA to the magnitude of the dependent variable. Next, a coefficient for GTclip placement, β, and for AML tether angle, γ, is added. Because these two variables are categorical, their coefficients are produced in a lookup table. For example, to calculate the estimated MVA after placement of a single central GTclip with a moderate AML tether angle, the coefficients for these two categories would be selected and inserted into Equation 4 for β and γ, respectively. Finally, an error term, ε, describes the model error.

These coefficients and overall statistical significance were computed for each factor and level using the Minitab GLM tool. Percent contribution to total sum of square variance was computed for AML tether angle, GTclip configuration, and baseline MAA. This contribution percentage represents the portion of variance in the dependent variables that can be attributed to each independent variable. In other words, this is the relative size of the effect that GTclip placement, AML tether angle, and MAA have on the decrease in MVA and increase in MVG.

4.6.2 Normality of Results and Equality of Variance

Bartlett's test and residual analysis was performed on all dependent variables. This is a test of the null hypothesis that observations come from normal distributions with the same variance. In all cases, the data was determined to be normally distributed with equal

variance. Thus, assumptions underpinning the GLM were not violated, and the model results were valid.

4.6.3 Post-Hoc Test

Using the “Comparison” tool in Minitab 18, multiple comparison via Tukey’s HSD procedure was conducted on the mean measurements of each group, to test differences in groups per the main effects of AML tether angle, GTclip configuration, and MAA. This provides the mean measurement (MVA, mean MVG, peak MVG, Total Fluid Force or Drag Force) and 95%CI for each combination of GTclip and AML tether angle at the mean MAA, allowing significant differences between groups to be detected.

CHAPTER 5: RESULTS

This section is arranged as follows. First, verification data on the GTclip bite profile and anterior mitral leaflet (AML) tether angle repeatability are presented. Next, the coefficients of the general linear models are presented, along with analysis of the effect of mitral annular area (MAA) on mean MV gradient (MVG), peak MVG, and MV area (MVA). This is followed by analysis of average values for mean/peak MVG and MVA at the mean MAA of 4.15 cm^2. Next, an analysis on the incidence of moderate mitral stenosis (MS) as a function of GTclip placement and AML tether angle is presented. Following the analysis of MS descriptors, mechanistic insights into forward flow obstruction are presented with the analysis of total fluid force and drag force on the MV apparatus at peak diastole. Finally, average baseline and post-clip values form this experiment are compared with those from clinical reports.

5.1 GTclip Bite Profile Verification

The leaflet bite profile of GTclip compared favorably to that of central MitraClip implantation in a patient. GTclip had a width of 5 mm, which created a bite with of approximately 6.5 mm, as measured in 3D echo and photogrammetry. In comparison, the width of MitraClip is 5 mm, and a leaflet bite width of approximately 6.8 mm was observed in a MitraClip patient. Furthermore, engineering studies have commonly simulated MitraClip by reproducing the leaflet bite profile of the device.[33, 58]

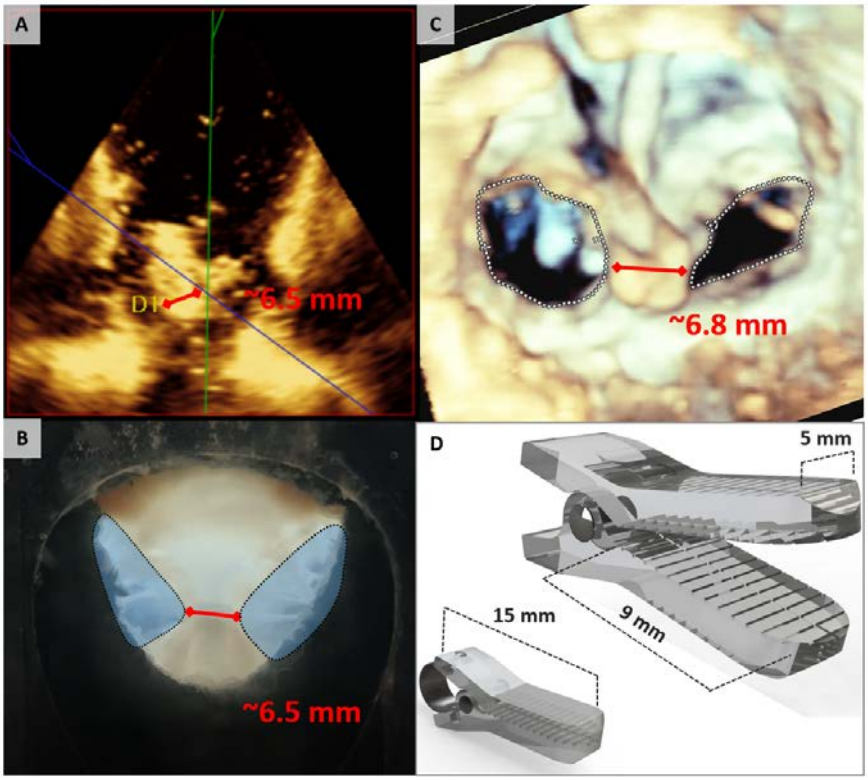

Figure 5-1 – Custom edge-to-edge clip (GTclip) leaflet bite profile verification. GTclip had a width of 5 mm, which created a bite with of approximately 6.5 mm, as measured in 3D echo and photogrammetry (A,B). In comparison, the width of MitraClip is 5 mm, and a leaflet bite width of approximately 6.8 mm was observed in a MitraClip patient (C). The dimensions of GTclip match those of MitraClip (D).

5.2 Leaflet Tethering Repeatability

Results in this section are reported as mean ± standard deviation. The AML tether angle repeatability experiment demonstrated that the applied methods created AML tether angles of 76.5±2.3°, 59.5±2.8°, and 47.6±2.0°. Subsequently, the tether angles achieved over the course of data collection were 75.2±2.3°, 60.7±2.1°, and 45.1±1.8°. The published human data[47], the results of the repeatability testing, and the mean AML tether angles observed during data collection are shown in Figure 5-2.

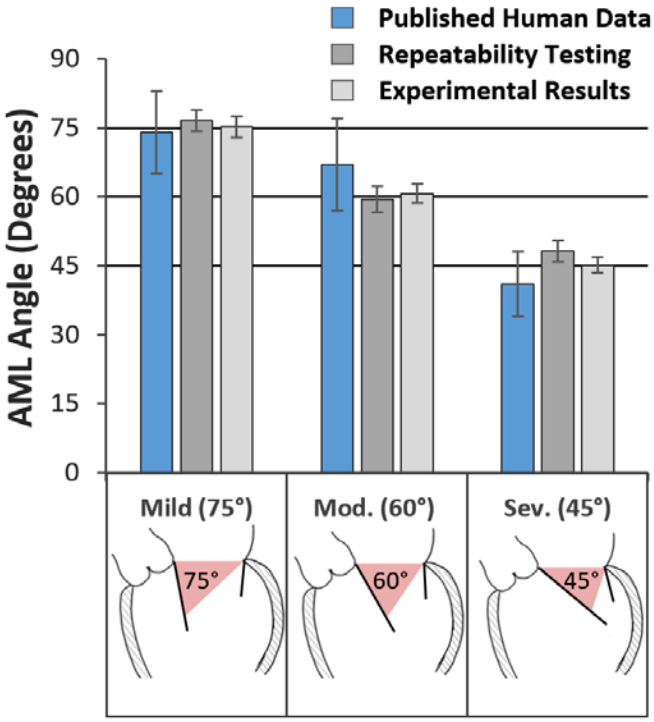

Figure 5-2 – Results of anterior mitral leaflet (AML) tethering repeatability test compared with published human data. Repeatability testing showed the AML tethering method reliably reproduced the desired condition, and AML tether angle results over the course of the study showed that the reliability was preserved. (AML tethering diagrams modified from Otsuji et al[47])

5.3 Factors Impacting Mitral Valve Area and Gradients

Results showed that AML tether angle, GTclip placement, and baseline annular area were significant factors impacting the measured mean MVG, peak MVG, and resulting MVA ($p<0.001$ for each factor and measurement). Factor significance, factor contributions and model coefficients are tabulated in

Table 5-1. Coefficients can be used to calculate mean and 95%CI values for the measurements. An example MVA calculation is shown in Equation 1,

$$MVA = k + (MAA - 4.0)\alpha + \beta + \gamma \quad (5)$$

where the constant coefficient, k, is summed with the GTclip coefficient, β, for the desired clip placement, and the AML coefficient, γ, for the desired AML angle. Finally, the product of MAA and the MAA coefficient, α, are added as shown to produce the MVA estimate given the selected inputs.

5.4 Effect of Baseline Mitral Annular Area

No significant post-procedural mean MVG (mean MVG >5mmHg) was observed in the two samples with baseline MAA≥4.4cm^2. In contrast, 13 incidents of mean MVG>5mmHg were observed in the samples with baseline MAA<4.1cm^2 (60 total experiments, frequency of 22%). Calculated based on the coefficient results shown in Table 5-1, the smallest MAA that resulted in mean MVG under 5mmHg was 4.7 cm^2, even in the presence of severe AML tethering and implantation of two GTclips. In other words, the mean MVG at baseline MAA of 4.7 cm^2, with severe AML tethering, and with central and commissural GTclips placed was 4.3±0.6 mmHg. Baseline MAA of 4.7cm^2 with severe AML tethering resulted in baseline pre-clip MVA by planimetry of 3.9±0.3cm^2.

Table 5-1 – Coefficients and contributions of factors affecting MV gradient (MVG) and area (MVA). All three factors, AML tether angle, GTclip placement, and baseline Mitral Annular Area (MAA), were found to significantly affect the three resulting measurements (mean MV gradient, peak MV gradient, and MV area), p>0.001 for all. The percent contributions show the relative importance of the effect of each factor on the measurement (contribution to total sum of square variance). Contribution of statistical error and small interaction contributions are not shown. Coefficient units are those of the corresponding measurement.

Main Factor / Term		**Contribution**	**Coefficient**	**95% CI**	**P-Value**
Mean MVG (mmHg)	**(R^2=0.83)**				
	Constant **(k)**		3.81	(3.71, 3.91)	<0.001
$MAA - 4.0\ cm^2$	**(α)**	**28.24%**	-1.55	(-1.80, -1.30)	**<0.001**
GTclip Placement	**(β)**	**39.06%**			**<0.001**
	None		-0.99	(-1.19, -0.80)	<0.001
	Single Comm.		-0.43	(-0.61, -0.24)	<0.001
	Single Central		0.01	(-0.17, 0.20)	0.887
	Dual Central		0.54	(0.37, 0.73)	<0.001
	Central+Comm.		0.86	(0.68, 1.05)	<0.001
AML Tether Angle	**(γ)**	**16.04%**			**<0.001**
	75 degrees		-0.33	(-0.47, -0.20)	<0.001
	60 degrees		-0.24	(-0.37, -0.11)	0.001
	45 degrees		0.57	(0.44, 0.70)	<0.001
Peak MVG (mmHg)	**(R^2=0.75)**				
	Constant **(k)**		6.91	(6.70, 7.12)	<0.001
$MAA - 4.0\ cm^2$	**(α)**	**24.37%**	-2.44	(-2.97, -1.90)	**<0.001**
GTclip Placement	**(β)**	**36.13%**			**<0.001**
	None		-1.50	(-1.92, -1.09)	<0.001
	Single Comm.		-0.78	(-1.18, -0.38)	<0.001
	Single Central		-0.10	(-0.50, 0.30)	0.627
	Dual Central		0.78	(0.38, 1.17)	<0.001
	Central+Comm.		1.61	(1.21, 2.01)	<0.001
AML Tether Angle	**(γ)**	**14.04%**			**<0.001**
	75 degrees		-0.54	(-0.82, -0.25)	<0.001
	60 degrees		-0.40	(-0.69, -0.12)	0.006
	45 degrees		0.94	(0.66, 1.22)	<0.001
MVA (cm^2)	**(R^2=0.95)**				
	Constant **(k)**		2.21	(2.16, 2.26)	<0.001
$MAA - 4.0\ cm^2$	**(α)**	**7.04%**	0.65	(0.53, 0.78)	**<0.001**
GTclip Placement	**(β)**	**80.65%**			**<0.001**
	None		1.53	(1.44, 1.62)	<0.001
	Single Comm.		-0.04	(-0.13, 0.05)	0.402
	Single Central		-0.13	(-0.22, -0.03)	0.009
	Dual Central		-0.49	(-0.59, -0.40)	<0.001
	Central+Comm.		-0.87	(-0.97, -0.78)	<0.001
AML Tether Angle	**(γ)**	**6.85%**			**<0.001**
	75 degrees		0.25	(0.18, 0.32)	<0.001
	60 degrees		0.07	(0.01, 0.14)	0.034
	45 degrees		-0.32	(-0.39, -0.26)	<0.001

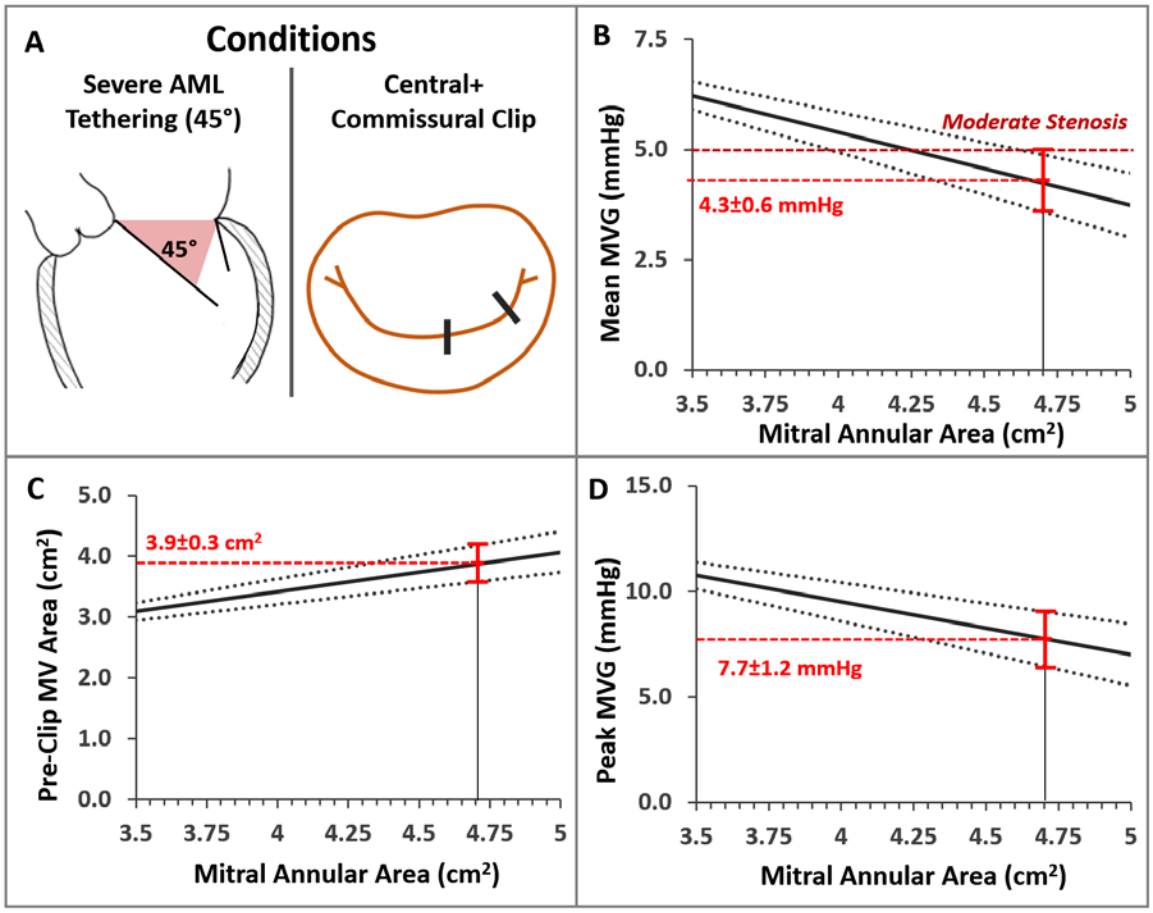

Figure 5-3 – Effect of baseline mitral annular area (MAA) on mitral stenosis with severe anterior mitral leaflet (AML) tethering, and placement of central and commissural GTclips. With conditions of severe AML tethering, and placement of central and commissural GTclips, mean and peak MVG values were estimated using the coefficients in Table 5-1.

5.5 Mitral Valve Area and Gradient at the Mean Mitral Annular Area

The mean MAA of all experiments was 4.15 cm^2. At this MAA, resulting MVA and MVG values (mean±95%CI) for all combinations of AML tether angle and GTclip placement are shown in Figure 5-4. Groups whose 95%CIs do not overlap are significantly different ($p<0.05$). The p-values for each possible comparison are tabulated in **Tables A-3, A-4, and A-5** of the Appendix A. In the case of mild AML tethering without clipping, the mean MVG was found to be 2.4±0.4 mmHg, while the mean MVA was 4.0±0.2 cm^2.

The severe AML tether angle alone caused an insignificant increase in mean MVG to 3.0±0.4 mmHg ($p=0.49$), but a significant decrease in MVA to 3.6±0.2 cm^2 ($p<0.05$). With commissural and central clips placed in the setting of a severe AML tether angle, the mean MVG was observed to be significantly greater at 5.7±0.6 mmHg ($p<0.001$), and four of six samples were moderately stenotic (mean MVG>5.0 mmHg). MVA in this case was found to be significantly smaller at 1.2±0.2 cm^2 ($p<0.001$). No significant differences were detected between the mild (75°) and moderate (60°) AML tether angles within each GTclip placement group, but larger-magnitude changes were observed in the severe (45°) group.

5.6 Change in Mitral Valve Area and Gradient from Baseline

Baseline MVA and MVG decreased and increased, respectively, as a function of AML tether severity. Taking the pre-clip results as a baseline, the elevation in MVG and decrease of MVA are shown for each clipped condition in Figure 5-4 (orange bars). AML tether angle was found to be a significant factor, but only in the mean and peak MVG, indicating that the *increase* in MVG from baseline to post-clip is significantly larger in the presence severe AML tethering (Figure 5-5A-C).

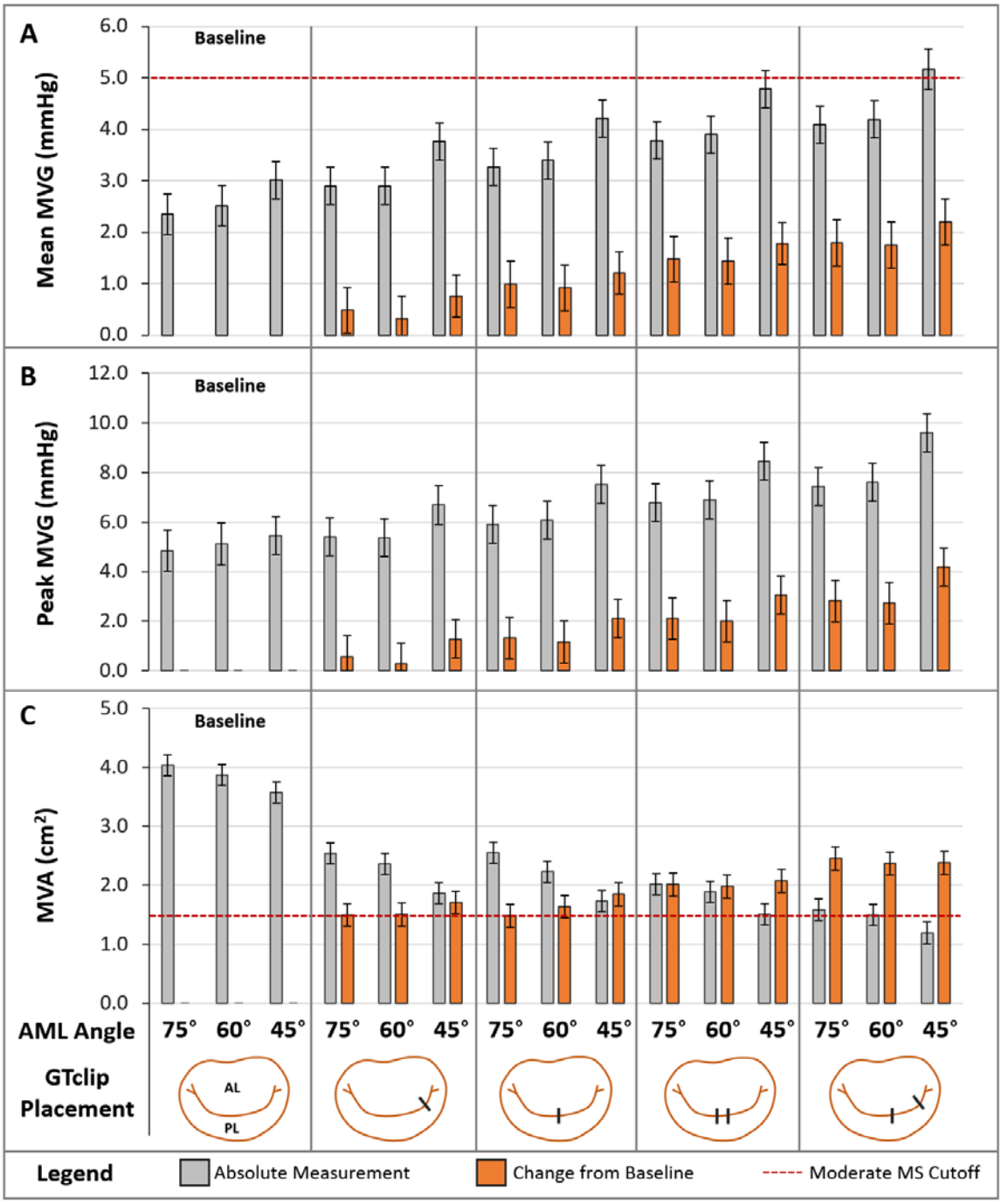

Figure 5-4 – Mean MV gradient (MVG), peak MVG, and MV area by GTclip placement and anterior mitral leaflet (AML) tether angle. Absolute mean and 95% confidence interval (95%CI) are shown via the grey bars for each group at a baseline annular area of 4.15 cm^2. Mean difference from pre-clip baseline with 95%CI is shown via the orange bars. The cutoff values for moderate MS are denoted by the red dotted lines. Statistically significant differences can be observed between groups whose 95%CIs do not overlap. A full table of p-values can be found in the Appendix A, Tables A-3, A-4 and A-5.

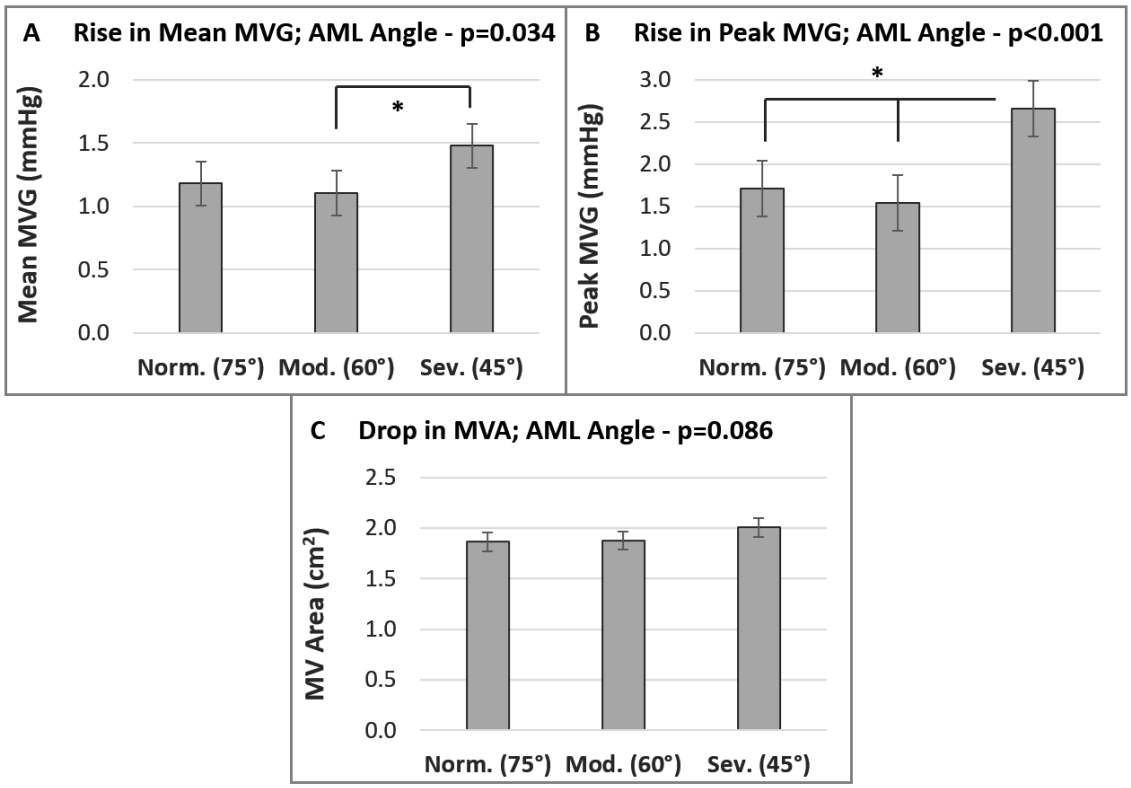

Figure 5-5 – Change from pre-clip baseline in mean MV gradient (MVG), peak MVG, and MV area (MVA) by anterior mitral leaflet (AML) tether angle. Mean values with 95% confidence interval (95%CI) computed at a baseline annular area of 4.15 cm^2. The effect of AL tether angle was significant for the rise both mean and peak MVG ($p<0.05$), but was not significant for the drop in MVA ($p=0.086$). * $p<0.05$

5.7 Rates of Mitral Stenosis by GTclip Placement and Anterior Mitral Leaflet Tether Angle

Across all experimental conditions, moderate MS (mean MVG>5mmHg) was created in 13 cases, 11 of which were found in the setting of severe AML tethering. Combined, mild and moderate AML tethering created MS at a frequency of 4%, while the frequency of MS for severe AML tethering was 46%. Clinical reports suggest avoiding placement of additional MitraClip if mean MVG is observed to be >4 mmHg.[44] Among all single-GTclip experiments, this threshold was exceeded only once (frequency of 8%) for

each of 75° and 60° AML angles, but five times (frequency of 42%) with severe AML tethering (Figure 5-6).

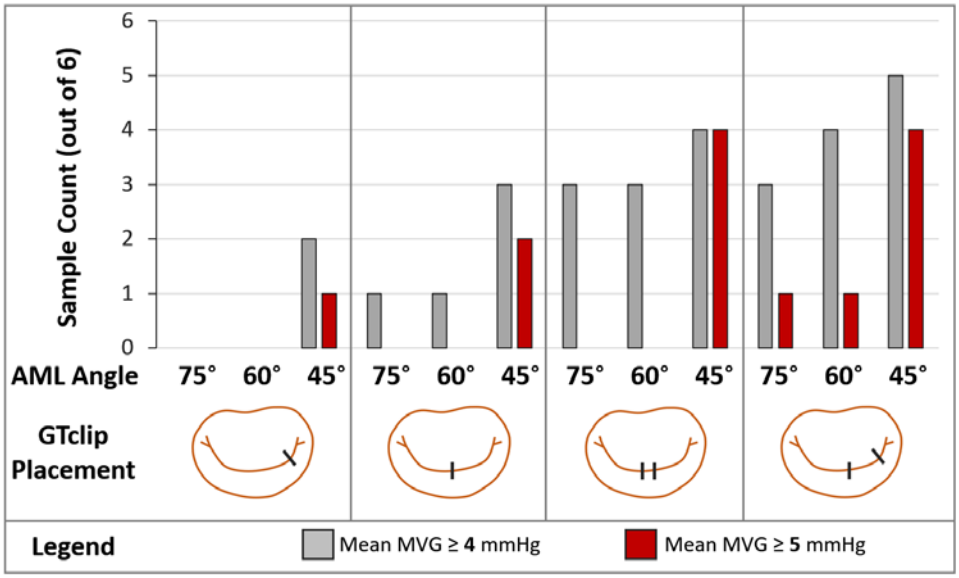

Figure 5-6 – Rates of moderate stenosis (MS) by GTclip placement and anterior mitral leaflet (AML) tether angle. Incidence of mean MVG≥4 mmHg (placement of additional GTclip not advised) and mean MVG≥5 mmHg (moderate MS) are shown in the grey bars and red bars, respectively. Total sample size was N=6 per condition.

5.8 Fluid Forces on the Mitral Valve Apparatus

The mean MAA of all experiments was 4.15 cm^2. At this MAA, resulting total fluid force and drag force values (mean±95%CI) for all combinations of AML tether angle and GTclip placement are shown in Figure 5-7. Groups whose 95%CIs do not overlap are significantly different ($p<0.05$). In the case of mild AML tethering without clipping, the drag force was found to be 0.37±0.06 N, while the total fluid force was 0.47±0.05 N. The severe AML tether angle alone caused a significant increase in drag force to 0.77±0.06 N ($p<0.001$), and a significant increase in total fluid force to 1.03±0.05 N ($p<0.001$). Without clipping, the total fluid force was found to be significantly greater than the drag force, in

the case of moderate and severe AML tethering ($p>0.05$ for both). However, after clipping, the fluid force and drag force were not significantly different, indicating that the force on the MV apparatus was dominated by drag after clipping ($p>0.05$ for all). In the most severe obstruction (commissural and central clips placed in the setting of a severe AML tether angle), the drag force was observed to 1.37±0.06 N, and the total fluid force was found to be 1.40±0.05 N. Both were significantly greater than their pre-clip counterparts ($p<0.001$ for both. In contrast to the MVA and MVG findings, significant differences in force were often observed between the mild and moderate tether angles. A full list of results, and p-values for each possible comparison are tabulated in Tables A-6 and A-7 of Appendix A.

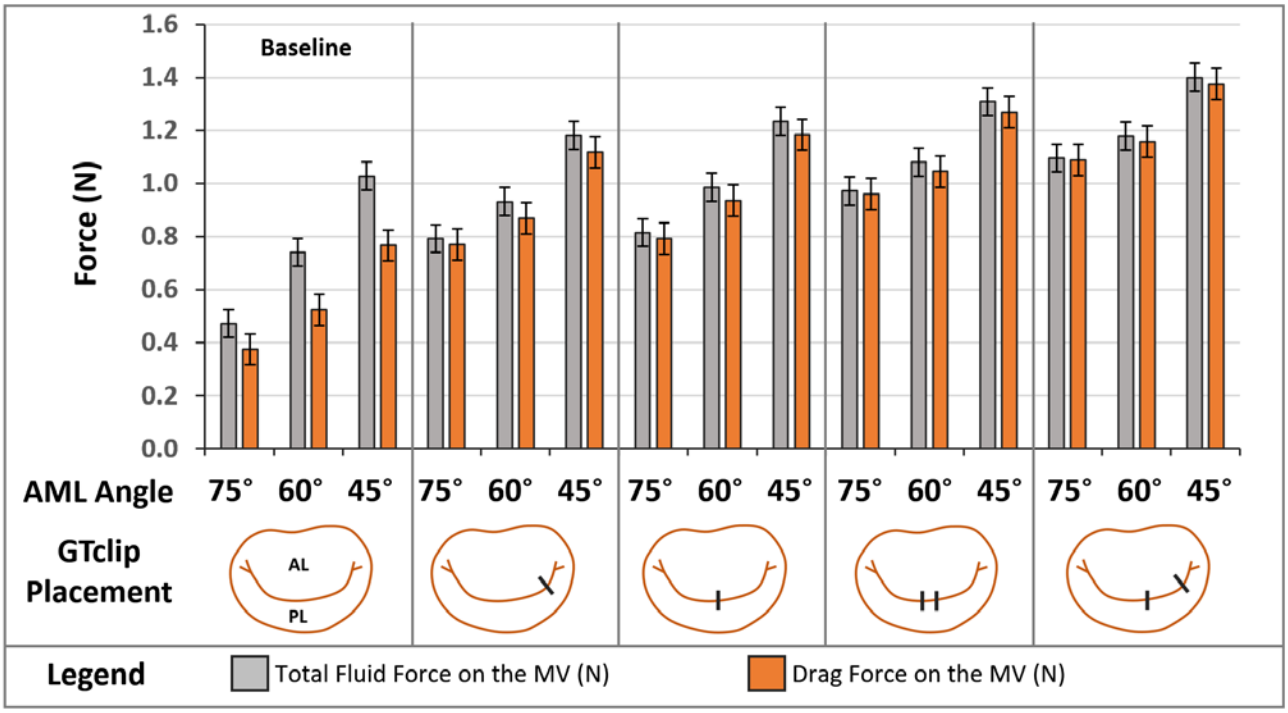

Figure 5-7 – Drag force and total fluid force on the MV apparatus by GTclip placement and anterior mitral leaflet (AML) tether angle. All values displayed as mean± 95% Confidence Interval (95%CI). Statistically significant differences can be observed between groups whose 95%CIs do not overlap. A full table of p-values can be found in Appendix A, tables A-6 and A-7.

5.9 MitraClip Clinical Comparison

In 12 FMR patients with varying degrees of leaflet tethering, Chan et al [48] report a baseline mean±95%CI MVA and mean MVG of 3.60±0.38 cm^2 and 2.20±0.83 mmHg, respectively. In the same study, after implantation of 1.3±0.7 MitraClip per patient, follow-up MVA and mean MVG were found to be 1.50±0.25 cm^2 and 4.90±1.02 mmHg, respectively. Averaged across AML tether angles, baseline MVA and mean MVG were found to be 3.83±0.32 cm^2 and 2.70±1.13 mmHg, respectively. Following placement of 1.5±0.5 GTclips, MVA and mean MVG values were found to be 1.92±0.46 cm^2 and 3.83±1.03 mmHg, respectively. Averaged across AML angle severity and GTclip placement, these results were not significantly different from a cohort of 12 patients with FMR ($p>0.05$ for all).[48] This indicates that the *in vitro* model presented herein was able to faithfully reproduce baseline and post-clip hemodynamics (Figure 5-8A,B).

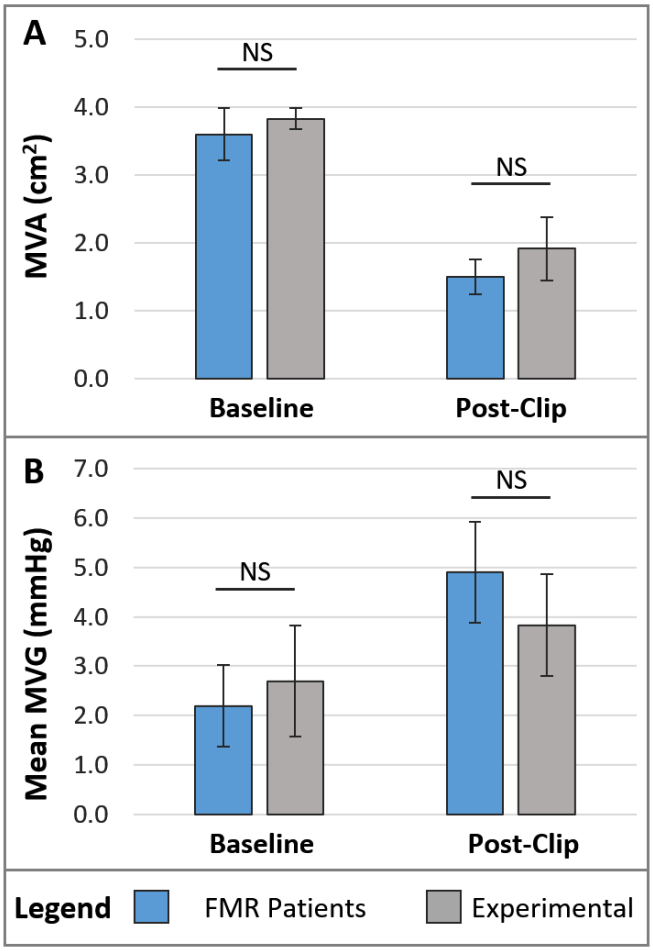

Figure 5-8 – Comparison of MV area (MVA) results and mean MV gradient (MVG) results to clinical data. Mean ± 95% Confidence Interval MVA and MVG are shown for a cohort of 12 FMR patients both pre- and post-clip.[48] No significant differences were detected. NS - p>0.05

CHAPTER 6: DISCUSSION

A clinically recognized suboptimal outcome of MitraClip treatment is the undesired creation of MS.[16, 25, 40, 41] A recently published report by Neuss et al has shown that significantly poorer long-term patient outcomes result with post-procedural mean MVG≥5 mmHg.[40, 42] Though undesired creation of MS may be a consequence of MitraClip therapy, well-established guidelines and practices are currently in-place to avoid such a result.[40, 44] Per the MitraClip IFU and EVEREST trials, MR patients with baseline MVA<4.0cm^2 are contraindicated for MitraClip treatment.[15] Per clinical practice, multiple MitraClip devices may be deployed to fully treat MR, but placement of additional devices may further reduce MVA and increase MVG. As a general guideline, additional clips are not placed if the patient has mean MVG≥4mmHg.[44]

Clinical evidence has suggested that AML tethering commonly seen in FMR may have an impact on the level of MS resulting from MitraClip implantation,[48] but studies on its effects are limited. To investigate this experimentally, MS severity after MitraClip in the setting of varied levels of AML tethering was quantified using an *in vitro* left heart model.[28, 50, 59] AML tethering was a significant factor affecting resulting MVG and MVA, as well as the change in those measures from pre-clip baseline.

6.1 Use of GTclip to Simulate MitraClip

MitraClip was simulated by replicating the size of the arms of the device with a custom edge-to-edge clip (GTclip). Qualitatively, the GTclip successfully approximated the leaflets at the site of implantation, and no incidence of leaflet damage or GTclip

detachment was observed. More quantitatively, the width of the leaflet bite of GTclip under echo imaging was compared to that of MitraClip. In-use, GTclip was found to closely match this bite profile. Though the method of action was different, the spring loaded GTclip was able to approximate the mitral leaflets in a sufficiently similar manner to a fully closed MitraClip device. This method of MitraClip simulation has also been previously established in computational models. Instead of creating a fully functioning model of MitraClip, the effect is simulated by creating two rigid rectangular gripping surfaces with the same dimensions as the MitraClip grippers, and using those to approximate the leaflets.[33, 58] This is analogous to the approach adopted in this work to simulate MitraClip implantation.

6.2 Insights into the Effects of AML Tethering

Within each GTclip group, no differences between AML tether angles of 75° and 60° were observed. However, much larger effects were observed at the severe AML tether angle of 45°. In the presence of severe AML tethering, a higher rate of moderate MS was observed, as compared to that in the presence of mild or moderate AML tethering (46% versus 4%, respectively). However, baseline MVA was significantly lower and baseline MVG was trending higher in the presence of severe AML tethering, so the increase in MVG and decrease in MVA after GTclip placement was computed. Mean and peak MVG was found to increase by a significantly larger magnitude in the presence of severe AML tethering, indicating that the AML tether severity may be an important factor for which to account.

AML tethering was found to have the dual effect of narrowing the MV orifice, and redirecting flow. The larger jet redirection angle may be a factor causing these large effects only at the most severe tether angles. To explore this, the drag force and total fluid force on the AML was computed using the simplified analysis of fluid force on a narrowing pipe bend. Both total fluid force and drag force were found to be significantly larger with severe AML tethering than with normal or moderate AML tethering, under all simulated GTclip positions ($p<0.05$). The fluid force on the MV apparatus may be balanced by the annulus, or the PMs. Additionally, loading on the AML may be balanced by the PML and posterior annulus via the GTclip, suggesting that the tension applied to the GTclip in diastole is greater with severe AML tethering. These observations suggest that the AML is under more tension at the most severe tether angles, and could explain the larger increase in MVG and decrease in MVA caused by GTclip placement under this condition.

6.3 Effect of GTclip Placement

The resulting MS severity largely depended on GTclip number, but was also affected by the positioning of GTclips. For example, resultant MVA after commissural GTclip placement was not significantly different from that after central GTclip placement, but mean MVG was significantly higher after central GTclip placement than after commissural GTclip placement ($p<0.05$). This could be attributed to the greater resistance to flow in the double-orifice case, despite the total MVA being equal. Differences between the double-clip cases were also observed. In the case of a double central GTclip placement, two distinct orifices were made. Placement of commissural and central GTclips created a single larger orifice, a smaller orifice between the GTclips, and a small orifice in the

commissure, which caused mean MVG to trend higher than that in the double central GTclip placement.

Clinical reports suggest avoiding placement of additional MitraClips if mean MVG is observed to be ≥4 mmHg.[44] Among single-GTclip experiments, a higher rate of mean MVG≥4mmHg was observed in the severe AML tethering group than in the combined mild and moderate group (42% versus 8%, respectively). In these cases, a "compromise" must be made between further reduction of MR and increase in MVG caused by placing additional GTclips. A similar finding has been reported clinically, with higher rates of "compromise" in patients with more severe AML tethering.[48]

The purpose of the 4 mmHg cutoff is to predict whether MS will be created after placement of an additional clip. However, the cutoff of 4 mmHg did not always accurately predict presence of MS after placement of additional GTclips. Some cases arose where placement of the second GTclip unexpectedly caused MS, along with some cases where this unexpectedly *did not* cause MS. First, commissural GTclip placement resulted in the lowest mean MVG, and an additional GTclip may often be permitted. However, mean MVG was highest in the central+commissural group. In four of 18 cases, mean MVG<4 mmHg resulted after commissural GTclip placement, followed by mean MVG≥5mmHg after placement of the second central GTclip. This occurred at a rate of 17% for mild and moderate AML tethering, and 33% for severe AML tethering. Because of the larger increase in mean MVG observed with severe AML tethering, and the larger increase observed from single commissural to central and commissural GTclip placement, this scenario led to a higher likelihood of unexpected MS.

Conversely, central GTclip placement resulted in higher mean MVG, and placement of an additional GTclip often may not be permitted. However, mean MVG was lower after double central GTclip than after central+commissural GTclip. In two of 18 cases, mean MVG≥4mmHg resulted after the first central GTclip, followed by mean MVG<5mmHg after the second central GTclip. Both were observed at AML excursion angles of 75° and 60°, respectively. Here, because of the smaller increase in mean MVG observed with mild and moderate AML tethering, and the smaller increase observed from single central to double central GTclip placement, the second GTclip did not cause MS, even though the cutoff was exceeded after the first GTclip.

6.4 Drag Force and Total Fluid Force on the Mitral Valve

Using control volume analysis and assuming the MV orifice to resemble an angled, narrowing pipe bend, the fluid force on the MV was calculated. In the case of the narrowing pipe bend, these forces correspond to the total thrust-block force, and the thrust block force in the direction of the inflow jet. In other words, the calculated force is the reaction force needed to keep the pipe bend (or MV) stationary. This in the case of the MV, this force must be balanced by the annulus and PMs, which are the two fixtures of the MV. The forces are made up of two components: the change in momentum of the flow from the inlet (annulus) to the outlet (past the leaflets), as well as the pressure force acting on the inlet control surface and the outlet control surface.

Interestingly, the total fluid force on the MV was significantly larger than the drag force only in the baseline pre-clip case. This indicates that, before GTclip is applied, a more substantial “lift” force, or force orthogonal to the inflow, is generated by the tethered AML.

However, once GTclip is applied, the substantial reduction in outlet area causes the total calculated fluid force to be dominated by drag force. After applying a single central GTclip in the setting of severe AML tethering, total force increased from 1.03±0.05 N to just 1.18±0.05 N. Drag force, however, increased from 0.77±0.06 N to 1.12±0.06 N. This could explain the larger contribution that GTclip has to the increase in forward flow obstruction, as compared to that of AML tethering. However, in combination, severe AML tethering and GTclip created clinically significant and larger magnitude forward flow obstruction.

6.5 Impact of Area on Gradients and Area Measurement Challenges

Several factors make MVA challenging to measure in MitraClip pre-procedural planning and evaluation: the three-dimensional MV orifice, the limited capacity for echocardiographic measurement of areas below 0.5cm^2, and the lack of a single, gold-standard measurement approach.[56] Nevertheless, MVA by planimetry has been found clinically to correlate with resulting rates of MS better than other methods (Pressure Half-Time MVA and 3D MVA by MVQ).[56] Therefore, all MVA measurements in this study were made by established planimetric guidelines.

The present *in vitro* investigation was limited by these same challenges. However, the GTLHS offered precise control of *annular* area (MAA). Accordingly, within the limitations of this system and the range of tested GTclip configurations, the statistical model identified 4.7 cm^2 as the MAA above which severe AML tethering did not cause Moderate MS (MVG≥5mmHg), even with placement of two GTclips (95% certainty). At this MAA, the model identified the mean baseline MVA to be 3.9±0.3cm^2 (at 45°), showing that, while MS was more frequent with severe AML tethering, the established MVA cutoff

of 4.0cm^2 was applicable for these findings. These results showed that MS occurred at the highest rate with severe AML tethering (45° diastolic excursion angle) *and* MVA<4.0cm^2.

6.6 Comparison to Existing Engineering Studies

Many *in vitro,* computational, and *in vivo* studies have been conducted to understand the efficacy of the E2E repair and MitraClip under certain conditions, the loading on the repair over the cardiac cycle, and the stress patterns in the leaflet caused by the repair.[26-29, 31, 33, 34, 38] Nielsen and colleagues measured force on E2E transducer simulating the Alfieri stitch in healthy and acute IMR animals.[31] They found a larger-magnitude force on the repair the diastolic phase of the cycle, indicating that the repair caused increased leaflet strain in diastole. However, the authors attributed this finding to the change in annular size over the cardiac cycle, and did not examine the force as a function of MVG. The current study calculated significantly higher force on the MV apparatus with severe AML tethering. This indicates that the tethered AML is under more strain in diastole, and may mean that more tension is being applied to the GTclip, than without tethering. Future studies are needed to directly measure the loading on the mitral leaflets as a function of MVG, and determine the implications for repair durability.

The previously mentioned studies have well characterized loading on the E2E repair, but parametric analyses on the effect of MitraClip on forward flow obstruction is lacking. Many of these studies simulated E2E repair or MitraClip on valves with MVA>5.5 cm^2; the data herein has shown that likelihood of elevated MVG and stenosis is greatest at baseline MVA~4.0cm^2 or less. Thus, clinically significant stenosis was likely not observed in these studies solely due to the size MV samples used. However, real-world use of

MitraClip treatment does include patients with FMR, leaflet tethering and smaller baseline MVA.[21, 48] Recently-published clinical reports have highlighted the importance of maintaining efficient forward flow following MV repair in general, and with MitraClip.[25, 40-42, 60] The present *in vitro* results in part address the need to understand the level of forward flow obstruction resulting from various simulated MitraClip placements, in the setting of varied leaflet tethering severity, and across a range of baseline mitral annular areas where MS may be a concern.

6.7 Clinical Implications

Appropriate selection of patients for successful treatment of MR with repair devices is critical to patient outcomes.[7] The original Alfieri stitch was originally not intended for use without a stabilizing annuloplasty ring, though MitraClip alone has been applied with great success.[13, 22] Use of the device to treat FMR, where disease of the ventricle is the underlying pathology, is now being studied in large-scale clinical trials. However, we have shown that altered leaflet functional, namely restricted leaflet opening in diastole, can have an effect on the resulting severity of mitral stenosis after simulated MitraClip. Recently, a similar clinical study from Kubota and colleagues has shown that severe leaflet tethering in FMR can cause MS in patients treated with mitral annuloplasty.[49] In the interest of improving patient outcomes, analogous investigations in transcatheter repair of FMR are necessary to determine the which FMR patients will be suitable not only for MitraClip, but also for new edge-to-edge repair clips such as PASCAL (Edwards Lifesciences, Irvine, CA USA).

6.8 Limitations

General limitations of the GT Left Heart Simulator have been previously described.[50] In addition, a prototype GTclip was used in place of a MitraClip. Though the MitraClip bite profile was carefully replicated, actual MitraClip dynamics may differ. Third, MR was not created in this model. MV samples were sufficiently robust, and coapted even with severe PM displacement. However, all findings were made during the diastolic phase of the cardiac cycle. Though presence of MR in systole may indeed affect the filling dynamics of the LV, LV inflow volume was held constant at 70 mL per beat for all experimental cases. Next, simplified and idealized analysis of fluid force on a narrowing pipe bend was assumed to estimate the force of fluid on the MV apparatus in diastole. This simplified assumption was made given the boundary conditions available. This actual force may vary, but comparisons and trends between conditions are valid. Finally, the MVA measurement challenges were noted above; nevertheless, the *in vitro* MVA and MVG results presented here agree well with those results observed in published clinical data.

CHAPTER 7: CONCLUSIONS

These results demonstrate that diastolic AML tethering can have a significant impact both on MS severity, as well as the increase in MV gradient after GTclip placement. Moderate MS occurred at a higher rate with severe AML tethering than with mild or moderate tethering (46% versus 4%, respectively). However, the model identified 4.7 cm^2 as the MAA above which severe AML tethering did not cause moderate MS (placement of up to two GTclips, 95% confidence). At this MAA, the mean baseline MVA was 3.9±0.3 cm^2 (at 45°), showing that, while MS was more frequent with severe AML tethering, the established MVA cutoff of 4.0 cm^2 was applicable for these findings.

A significant increase in force on the MV apparatus was also observed with severe AML tethering and MS. This increased force creates an increased diastolic tension in the mitral leaflets. Implications of this on long-term durability are not yet clear, but altered leaflet stress has been related to tissue remodeling.

These conclusions are derived from *in vitro* testing, which compared favorably to baseline and post-clip results in FMR patients. Severity of AML tethering may be an important criterion in selecting patients for edge-to-edge repair.

CHAPTER 8: FUTURE WORK

Transcatheter mitral valve repair is an ever-growing and ever-challenging endeavor.[7] MitraClip and transcatheter edge-to-edge repair are the safest available options, but lack effectiveness; MR often cannot be completely eliminated and patients are often left with MR levels as high as 2+.[61] Toward the goal of complete MR reduction using this technique, further investigations into the effectiveness of edge-to-edge repair must take place. Additionally, increasing focus and attention is being paid to "The Forgotten Valve" or the tricuspid valve.[62] Further investigations into MitraClip efficacy in treating tricuspid regurgitation (TR) could provide valuable data at a much earlier stage of device use.

8.1 MitraClip in FMR

8.1.1 Leaflet Strain/Damage

The edge-to-edge repair devices places stress on the mitral leaflets after deployment. Cases of leaflet perforation and MitraClip detachment have been reported.[63] It is unclear if leaflet tethering characteristic of FMR may cause a greater likelihood of this adverse event occurring. Investigation into effect of MitraClip placement on MV leaflet stress/strain in the setting of FMR and leaflet tethering could provide useful information.

8.1.2 Efficacy of MitraClip in Type IIIb Systolic Tethering

Under conditions of Type IIIb systolic tethering and severe FMR, effectiveness of MitraClip may be highly dependent on the positioning of the device. Because the MV

apparatus is under a larger tension, the effect of the MitraClip on MV coaptation may differ from conventional use in DMR patients. Investigation of optimal device placement in the setting of varied FMR etiologies would shed light on this issue.

8.1.3 Towards a Predictive Model and Decision Making Tool

The statistical model presented herein can readily be applied to clinical data in the same way. Incorporating the same variables in a clinical model could yield a robust tool which may be applicable in assessment of patient suitability for MitraClip treatment.

8.2 MitraClip in the Tricuspid Valve

8.2.1 Use of MitraClip in FTR

Use of MitraClip to treat FTR is currently gaining clinical traction, but many issues, including patient selection and FTR quantification remain.[62] Recent studies have investigated effectiveness of MitraClip in reducing FTR using an *ex vivo* model.[64] Additional parametric investigations of use of MitraClip in the right heart may shed light on patient selection and effectiveness criteria.

APPENDIX A. SUPPLEMENTARY DATA

A-1 Summary of AML tether angles observed in clinical human data,[47] in a pilot repeatability test, and over the course of all experiments (N=6). This data was used to create Figure 5-2.

Summary of AML Tether Angles (Degrees)				
Angle Target	Measure	Pilot	Experimental	Clinical
75 Degrees (Mild)	Mean	76.55	75.20	74.00
	SD	2.33	2.25	9.00
60 Degrees (Moderate)	Mean	59.47	60.73	67.00
	SD	2.80	2.05	10.00
45 Degrees (Severe)	Mean	48.10	45.13	41.00
	SD	2.30	1.76	7.00

A-2 Estimations and 95% confidence intervals (95%CI) for MV area, and mean/peak MV gradient.

Table A-2-1 – Estimates and 95% confidence intervals (CI) for pre-GTclip mitral valve area (MVA) under severe anterior mitral leaflet (AML) tethering. Additionally, mean MVG and peak MVG estimates and 95%CIs after placement of central and commissural GTclips with severe AML tethering. All values calculated as a function of mitral annular area (MAA). Data used for Figure 5-3 C-D.

Estimations and 95% Confidence Intervals									
	Baseline MVA (cm^2)			Mean Grad (mmHg)			Peak Grad (mmHg)		
MAA (cm^2)	Est.	+CI	-CI	Est.	+CI	-CI	Est.	+CI	-CI
3.5	3.1	3.2	2.9	6.2	6.5	5.9	10.8	11.4	10.1
3.6	3.2	3.3	3.0	6.1	6.4	5.7	10.5	11.2	9.8
3.7	3.2	3.4	3.1	5.9	6.3	5.5	10.3	11.0	9.5
3.8	3.3	3.5	3.1	5.7	6.1	5.3	10.0	10.8	9.2
3.9	3.4	3.6	3.2	5.6	6.0	5.1	9.8	10.6	8.9
4	3.4	3.6	3.2	5.4	5.9	4.9	9.5	10.4	8.6
4.1	3.5	3.7	3.3	5.2	5.7	4.7	9.3	10.2	8.3
4.2	3.6	3.8	3.3	5.1	5.6	4.6	9.0	10.0	8.0
4.3	3.6	3.9	3.4	4.9	5.4	4.4	8.8	9.8	7.7
4.4	3.7	3.9	3.4	4.7	5.3	4.2	8.5	9.6	7.4
4.5	3.7	4.0	3.5	4.6	5.2	4.0	8.2	9.4	7.1
4.6	3.8	4.1	3.5	4.4	5.0	3.8	8.0	9.2	6.8
4.7	3.9	4.2	3.6	4.2	4.9	3.6	7.7	9.0	6.5
4.8	3.9	4.3	3.6	4.1	4.7	3.4	7.5	8.8	6.1
4.9	4.0	4.3	3.7	3.9	4.6	3.2	7.2	8.7	5.8
5	4.1	4.4	3.7	3.7	4.5	3.0	7.0	8.5	5.5

Table A-2-2 – Coefficients and 95% confidence intervals pulled from

Table 5-1, which were used to calculate the values in Table A-2-1 as demonstrated in Equation 5. All coefficient units are in the units of their respective measurements.

Coefficients					
Measure		Const	MAA	Clip	AML
Mean MVG	val	3.8129	-1.658	0.953	0.6312
	-e	3.705	-1.932	0.749	0.4872
	+e	3.921	-1.384	1.157	0.7753
Peak MVG	val	6.875	-2.505	1.647	0.98
	-e	6.659	-3.052	1.24	0.692
	+e	7.09	-1.958	2.055	1.268
MVA	val	2.21	0.65	1.53	-0.32
	-e	2.16	0.53	1.44	-0.39
	+e	2.26	0.78	1.62	-0.25

A-3 Mean MV Gradient and Significant Differences at Mitral Annular Area of 4.15cm^2

Table A-3 – Mean MV gradient values displayed in Figure 5-4A. The top section of the table shows the mean MVG values along with SE and 95%CI for each combination of GTclip placement and AML tether angle. The second section shows the change in these values from baseline pre-clip. The third section shows a count of the number of MV samples found have MVG>4mmHg in the first row and the number that were moderately stenotic (MVG>5mmHg) in the second row (N=6 per column). The final section of the table shows the p value for each possible comparison of row v. column. Significant p values are highlighted red.

GTclip Placement	No Clip			Single Commissure			Single Central			Double Central			Central+ Commissure		
Tether Angle (Degrees)	**75**	**60**	**45**	**75**	**60**	**45**	**75**	**60**	**45**	**75**	**60**	**45**	**75**	**60**	**45**
Mean Gradient (mmHg)	2.4	2.5	3.0	2.9	2.9	3.8	3.3	3.4	4.2	3.8	3.9	4.8	4.1	4.2	5.2
Std. Error	0.2	0.2	0.2	0.2	0.2	0.2	0.2	0.2	0.2	0.2	0.2	0.2	0.2	0.2	0.2
95% Conf. Interval	0.4	0.4	0.4	0.4	0.4	0.4	0.4	0.4	0.4	0.4	0.4	0.4	0.4	0.4	0.4
Mean increase from baseline (mmHg)				0.5	0.3	0.8	1.0	0.9	1.2	1.5	1.4	1.8	1.8	1.7	2.2
Std. Error				0.2	0.2	0.2	0.2	0.2	0.2	0.2	0.2	0.2	0.2	0.2	0.2
95% Conf. Interval				0.4	0.4	0.4	0.4	0.4	0.4	0.4	0.4	0.4	0.4	0.4	0.4
No. >4mmHg (of 6)	0	0	0	0	0	2	1	1	3	3	3	4	3	4	5
No. Stenotic (>5mmHg) (of 6)	0	0	0	0	0	1	0	0	2	0	0	4	1	1	4
Freq. Stenotic	0.0	0.0	0.0	0.0	0.0	0.2	0.0	0.0	0.3	0.0	0.0	0.7	0.2	0.2	0.7
P Values (Column v. Row)															
No Clip, 75 Deg.		**1.000**	**0.494**	**0.790**	**0.788**	**0.000**	**0.076**	**0.021**	**0.000**	**0.000**	**0.000**	**0.000**	**0.000**	**0.000**	**0.000**
No Clip, 60 Deg.			**0.868**	**0.983**	**0.983**	**0.002**	**0.288**	**0.107**	**0.000**	**0.001**	**0.000**	**0.000**	**0.000**	**0.000**	**0.000**
No Clip, 45 Deg.				**1.000**	**1.000**	**0.246**	**1.000**	**0.981**	**0.002**	**0.199**	**0.073**	**0.000**	**0.008**	**0.002**	**0.000**
Single Commissure, 75 Deg.					**1.000**	**0.086**	**0.982**	**0.846**	**0.000**	**0.066**	**0.020**	**0.000**	**0.002**	**0.000**	**0.000**
Single Commissure, 60 Deg.						**0.087**	**0.983**	**0.848**	**0.000**	**0.066**	**0.020**	**0.000**	**0.002**	**0.000**	**0.000**
Single Commissure, 45 Deg.							**0.851**	**0.984**	**0.914**	**1.000**	**1.000**	**0.015**	**0.994**	**0.941**	**0.000**
Single Central, 75 Deg.								**1.000**	**0.037**	**0.797**	**0.515**	**0.000**	**0.126**	**0.047**	**0.000**
Single Central, 60 Deg.									**0.128**	**0.970**	**0.827**	**0.000**	**0.339**	**0.157**	**0.000**
Single Central, 45 Deg.										**0.945**	**0.996**	**0.669**	**1.000**	**1.000**	**0.054**
Double Central, 75 Deg.											**1.000**	**0.020**	**0.997**	**0.964**	**0.000**
Double Central, 60 Deg.												**0.067**	**1.000**	**0.998**	**0.001**
Double Central, 45 Deg.													**0.350**	**0.609**	**0.985**
Central+Comm, 75 Deg.														**1.000**	**0.015**
Central+Comm, 60 Deg.															**0.043**
Central+Comm, 45 Deg.															

A-4 Peak MV Gradient and Significant Differences at Mitral Annular Area of 4.15cm^2

Table A-4 – Peak MV gradient values displayed in Figure 5-4B. The top section of the table shows the mean values along with SE and 95%CI for each combination of GTclip placement and AML tether angle. The second section shows the change in these values from baseline pre-clip. The final section of the table shows the p value for each possible comparison of row v. column. Significant p values are highlighted red.

GTclip Placement	No Clip			Single Commissure			Single Central			Double Central			Central+ Commissure		
Tether Angle (Degrees)	**75**	**60**	**45**	**75**	**60**	**45**	**75**	**60**	**45**	**75**	**60**	**45**	**75**	**60**	**45**
Peak Gradient (mmHg)	4.9	5.1	5.5	5.4	5.4	6.7	5.9	6.1	7.5	6.8	6.9	8.5	7.4	7.6	9.6
Std. Error	0.4	0.4	0.4	0.4	0.4	0.4	0.4	0.4	0.4	0.4	0.4	0.4	0.4	0.4	0.4
95% Conf. Interval	0.8	0.8	0.8	0.8	0.8	0.8	0.8	0.8	0.8	0.8	0.8	0.8	0.8	0.8	0.8
Mean increase from baseline (mmHg)				0.6	0.3	1.3	1.3	1.2	2.1	2.1	2.0	3.1	2.8	2.7	4.2
Std. Error				0.4	0.4	0.4	0.4	0.4	0.4	0.4	0.4	0.4	0.4	0.4	0.4
95% Conf. Interval				0.8	0.8	0.8	0.8	0.8	0.8	0.8	0.8	0.8	0.8	0.8	0.8
P Values (Column v. Row)															
No Clip, 75 Deg.		1.000	0.999	1.000	1.000	0.120	0.871	0.718	0.002	0.082	0.047	0.000	0.003	0.001	0.000
No Clip, 60 Deg.			1.000	1.000	1.000	0.317	0.986	0.938	0.008	0.237	0.151	0.000	0.012	0.005	0.000
No Clip, 45 Deg.				1.000	1.000	0.634	1.000	0.998	0.027	0.522	0.376	0.000	0.041	0.017	0.000
Single Commissure, 75 Deg.					1.000	0.567	1.000	0.995	0.020	0.456	0.318	0.000	0.031	0.013	0.000
Single Commissure, 60 Deg.						0.529	1.000	0.993	0.017	0.420	0.288	0.000	0.027	0.011	0.000
Single Commissure, 45 Deg.							0.985	0.998	0.974	1.000	1.000	0.117	0.990	0.944	0.000
Single Central, 75 Deg.								1.000	0.231	0.963	0.902	0.002	0.308	0.167	0.000
Single Central, 60 Deg.									0.392	0.994	0.975	0.005	0.492	0.301	0.000
Single Central, 45 Deg.										0.991	0.998	0.927	1.000	1.000	0.024
Double Central, 75 Deg.											1.000	0.169	0.997	0.975	0.000
Double Central, 60 Deg.												0.266	1.000	0.994	0.001
Double Central, 45 Deg.													0.870	0.964	0.749
Central+Comm, 75 Deg.														1.000	0.015
Central+Comm, 60 Deg.															0.037
Central+Comm, 45 Deg.															

A-5 Mitral Valve Area and Significant Differences at Mitral Annular Area of 4.15cm^2

Table A-5 – MV area values displayed in Figure 5-4C. The top section of the table shows the mean values along with SE and 95%CI for each combination of GTclip placement and AML tether angle. The second section shows the change in these values from baseline pre-clip. The final section of the table shows the p value for each possible comparison of row v. column. Significant p values are highlighted red.

GTclip Placement	No Clip			Single Commissure			Single Central			Double Central			Central+Commissure		
Tether Angle (Degrees)	**75**	**60**	**45**	**75**	**60**	**45**	**75**	**60**	**45**	**75**	**60**	**45**	**75**	**60**	**45**
MVA (cm^2)	4.0	3.9	3.6	2.5	2.4	1.9	2.6	2.2	1.7	2.0	1.9	1.5	1.6	1.5	1.2
Std. Error	0.1	0.1	0.1	0.1	0.1	0.1	0.1	0.1	0.1	0.1	0.1	0.1	0.1	0.1	0.1
95% Conf. Interval	0.2	0.2	0.2	0.2	0.2	0.2	0.2	0.2	0.2	0.2	0.2	0.2	0.2	0.2	0.2
Mean increase from baseline (cm^2)				1.5	1.5	1.7	1.5	1.6	1.8	2.0	2.0	2.1	2.5	2.4	2.4
Std. Error				0.1	0.1	0.1	0.1	0.1	0.1	0.1	0.1	0.1	0.1	0.1	0.1
95% Conf. Interval				0.2	0.2	0.2	0.2	0.2	0.2	0.2	0.2	0.2	0.2	0.2	0.2
P Values (Column v. Row)															
No Clip, 75 Deg.		0.992	0.045	0.000	0.000	0.000	0.000	0.000	0.000	0.000	0.000	0.000	0.000	0.000	0.000
No Clip, 60 Deg.			0.633	0.000	0.000	0.000	0.000	0.000	0.000	0.000	0.000	0.000	0.000	0.000	0.000
No Clip, 45 Deg.				0.000	0.000	0.000	0.000	0.000	0.000	0.000	0.000	0.000	0.000	0.000	0.000
Single Commissure, 75 Deg.					0.989	0.000	1.000	0.509	0.000	0.011	0.000	0.000	0.000	0.000	0.000
Single Commissure, 60 Deg.						0.019	0.977	0.999	0.001	0.349	0.030	0.000	0.000	0.000	0.000
Single Commissure, 45 Deg.							0.000	0.284	0.999	0.997	1.000	0.273	0.672	0.236	0.000
Single Central, 75 Deg.								0.429	0.000	0.008	0.000	0.000	0.000	0.000	0.000
Single Central, 60 Deg.									0.019	0.955	0.373	0.000	0.000	0.000	0.000
Single Central, 45 Deg.										0.627	0.996	0.919	0.998	0.892	0.007
Double Central, 75 Deg.											0.999	0.012	0.073	0.010	0.000
Double Central, 60 Deg.												0.201	0.566	0.171	0.000
Double Central, 45 Deg.													1.000	1.000	0.502
Central+Comm, 75 Deg.														1.000	0.165
Central+Comm, 60 Deg.															0.554
Central+Comm, 45 Deg.															

A-6 Fluid Force on the Mitral Valve and Significant Differences

Table A-6 – Fluid force and drag force values displayed in Figure 5-7. The top section of the table shows the mean total fluid force values along with SE and 95%CI for each combination of GTclip placement and AML tether angle. The final section of the table shows the p value for each possible comparison of row v. column. Significant p values are highlighted red.

GTclip Placement	No Clip			Single Commissure			Single Central			Double Central			Central+Commissure		
Tether Angle (Degrees)	**75**	**60**	**45**	**75**	**60**	**45**	**75**	**60**	**45**	**75**	**60**	**45**	**75**	**60**	**45**
Total Force (N)	0.47	0.74	1.03	0.79	0.93	1.18	0.81	0.99	1.23	0.97	1.08	1.31	1.10	1.18	1.40
Std. Error	0.03	0.03	0.03	0.03	0.03	0.03	0.03	0.03	0.03	0.03	0.03	0.03	0.03	0.03	0.03
95% Conf. Interval	0.05	0.05	0.05	0.05	0.05	0.05	0.05	0.05	0.05	0.05	0.05	0.05	0.05	0.05	0.05
P Values (Column v. Row)															
No Clip, 75 Deg.		0.000	0.000	0.000	0.000	0.000	0.000	0.000	0.000	0.000	0.000	0.000	0.000	0.000	0.000
No Clip, 60 Deg.			0.000	0.987	0.000	0.000	0.818	0.000	0.000	0.000	0.000	0.000	0.000	0.000	0.000
No Clip, 45 Deg.				0.000	0.427	0.010	0.000	0.998	0.000	0.975	0.986	0.000	0.891	0.012	0.000
Single Commissure, 75 Deg.					0.031	0.000	1.000	0.000	0.000	0.001	0.000	0.000	0.000	0.000	0.000
Single Commissure, 60 Deg.						0.000	0.144	0.982	0.000	0.999	0.015	0.000	0.004	0.000	0.000
Single Commissure, 45 Deg.							0.000	0.000	0.981	0.000	0.346	0.076	0.628	1.000	0.000
Single Central, 75 Deg.								0.002	0.000	0.007	0.000	0.000	0.000	0.000	0.000
Single Central, 60 Deg.									0.000	1.000	0.457	0.000	0.217	0.000	0.000
Single Central, 45 Deg.										0.000	0.008	0.835	0.030	0.974	0.003
Double Central, 75 Deg.											0.236	0.000	0.091	0.000	0.000
Double Central, 60 Deg.												0.000	1.000	0.384	0.000
Double Central, 45 Deg.													0.000	0.065	0.490
Central+Comm, 75 Deg.														0.670	0.000
Central+Comm, 60 Deg.															0.000
Central+Comm, 45 Deg.															

A-7 Drag Force on the Mitral Valve and Significant Differences

Table A-7 – Drag force values displayed in Figure 5-7. The top section of the table shows the mean drag force values along with SE and 95%CI for each combination of GTclip placement and AML tether angle. The drag force represents the opposing force in the direction of mitral inflow for these combinations. The final section of the table shows the p value for each possible comparison of row v. column. Significant p values are highlighted red.

GTclip Placement	No Clip			Single Commissure			Single Central			Double Central			Central+Commissure		
Tether Angle (Degrees)	**75**	**60**	**45**	**75**	**60**	**45**	**75**	**60**	**45**	**75**	**60**	**45**	**75**	**60**	**45**
Drag (N)	0.37	0.52	0.77	0.77	0.87	1.12	0.79	0.93	1.18	0.96	1.05	1.27	1.09	1.16	1.37
Std. Error	0.03	0.03	0.03	0.03	0.03	0.03	0.03	0.03	0.03	0.03	0.03	0.03	0.03	0.03	0.03
95% Conf. Interval	0.06	0.06	0.06	0.06	0.06	0.06	0.06	0.06	0.06	0.06	0.06	0.06	0.06	0.06	0.06
P Values (Column v. Row)															
No Clip, 75 Deg.		0.051	0.000	0.000	0.000	0.000	0.000	0.000	0.000	0.000	0.000	0.000	0.000	0.000	0.000
No Clip, 60 Deg.			0.000	0.000	0.000	0.000	0.000	0.000	0.000	0.000	0.000	0.000	0.000	0.000	0.000
No Clip, 45 Deg.				1.000	0.509	0.000	1.000	0.014	0.000	0.002	0.000	0.000	0.000	0.000	0.000
Single Commissure, 75 Deg.					0.563	0.000	1.000	0.017	0.000	0.003	0.000	0.000	0.000	0.000	0.000
Single Commissure, 60 Deg.						0.000	0.893	0.968	0.000	0.721	0.008	0.000	0.000	0.000	0.000
Single Commissure, 45 Deg.							0.000	0.004	0.963	0.029	0.926	0.045	1.000	1.000	0.000
Single Central, 75 Deg.								0.082	0.000	0.015	0.000	0.000	0.000	0.000	0.000
Single Central, 60 Deg.									0.000	1.000	0.392	0.000	0.036	0.000	0.000
Single Central, 45 Deg.										0.000	0.098	0.796	0.648	1.000	0.002
Double Central, 75 Deg.											0.789	0.000	0.165	0.001	0.000
Double Central, 60 Deg.												0.000	0.999	0.368	0.000
Double Central, 45 Deg.													0.006	0.378	0.457
Central+Comm, 75 Deg.														0.953	0.000
Central+Comm, 60 Deg.															0.000
Central+Comm, 45 Deg.															

A-8 Data for Experimental Results Compared with Published Human Results

Table A-8 – Baseline and post-clip MV area and mean MV gradient values for the experimental results presented herein, compared with those reported in Chan et al.[48] Values used to produce Figure 5-8.

			Baseline	After Clip
MVA (cm^2)	CFML	Mean	3.83	1.92
		SD	0.31	0.44
		95% CI	0.15	0.46
	Chan et al	Mean	3.60	1.50
		SD	0.60	0.40
		96% CI	0.38	0.25
MVG (mmHg)	CFML	Mean	2.47	3.88
		SD	1.14	1.06
		95% CI	1.20	1.11
	Chan et al	Mean	2.20	4.90
		SD	1.30	1.60
		95% CI	0.83	1.02

A-9 Tabulated Data for All Experiments

A-9.1 Tabulated Data Sections

The following master data table is split into six sections. The sections are assembled as follows to create the master data table in its entirety. The tables on pages 64-69 do not fit on one page, and are divided and arranged as shown below. Statistical outliers are marked red, and were omitted from analysis

Section A1	**Section B1**	**Section C1**
Section A2	**Section B2**	**Section C2**

A-9.2 Table Section A1

Tether angle legend: 1 – 75; 2 – 60; 3 – 45 GTclip No. legend: 1 – No Clip; 2 – Single Commissure; 3 – Single Central; 4 – Double Central; 5 – Commissure+Central

Name	Factor Code	Experiment	GTclip No.	Tether Angle	MAA (cm^2)	Cardiac Output (lpm)
No Clip Tether75	111	1	1	1	3.90	5.046
No Clip Tether60	112	1	1	2	3.90	5.000
No Clip Tether45	113	1	1	3	3.90	4.997
SingleComm Tether75	121	1	2	1	3.90	5.051
SingleComm Tether60	122	1	2	2	3.90	5.009
SingleComm Tether45	123	1	2	3	3.90	5.084
SingleCentral Tether75	131	1	3	1	3.90	5.066
SingleCentral Tether60	132	1	3	2	3.90	5.078
SingleCentral Tether45	133	1	3	3	3.90	5.048
DualCentral Tether75	141	1	4	1	3.90	5.023
DualCentral Tether60	142	1	4	2	3.90	5.084
DualCentral Tether45	143	1	4	3	3.90	5.083
CentralComm Tether75	151	1	5	1	3.90	5.060
CentralComm Tether60	152	1	5	2	3.90	5.150
CentralComm Tether45	153	1	5	3	3.90	5.142
No Clip Tether75	211	2	1	1	4.37	5.069
No Clip Tether60	212	2	1	2	4.37	5.034
No Clip Tether45	213	2	1	3	4.37	5.034
SingleComm Tether75	221	2	2	1	4.37	5.080
SingleComm Tether60	222	2	2	2	4.37	5.074
SingleComm Tether45	223	2	2	3	4.37	5.032
SingleCentral Tether75	231	2	3	1	4.37	4.996
SingleCentral Tether60	232	2	3	2	4.37	5.009
SingleCentral Tether45	233	2	3	3	4.37	5.087
DualCentral Tether75	241	2	4	1	4.37	5.063
DualCentral Tether60	242	2	4	2	4.37	5.039
DualCentral Tether45	243	2	4	3	4.37	5.077
CentralComm Tether75	251	2	5	1	4.37	5.037
CentralComm Tether60	252	2	5	2	4.37	5.034
CentralComm Tether45	253	2	5	3	4.37	4.992
No Clip Tether75	311	3	1	1	3.63	5.067
No Clip Tether60	312	3	1	2	3.63	5.040
No Clip Tether45	313	3	1	3	3.63	5.106
SingleComm Tether75	321	3	2	1	3.63	4.964
SingleComm Tether60	322	3	2	2	3.63	4.960
SingleComm Tether45	323	3	2	3	3.63	4.957
SingleCentral Tether75	331	3	3	1	3.63	5.111
SingleCentral Tether60	332	3	3	2	3.63	4.995
SingleCentral Tether45	333	3	3	3	3.63	4.975
DualCentral Tether75	341	3	4	1	3.63	4.965
DualCentral Tether60	342	3	4	2	3.63	4.941
DualCentral Tether45	343	3	4	3	3.63	4.997
CentralComm Tether75	351	3	5	1	3.63	5.025
CentralComm Tether60	352	3	5	2	3.63	5.059
CentralComm Tether45	353	3	5	3	3.63	5.129

A-9.3 Table Section A2

No Clip Tether75	411	4	1	1	3.99	4.938
No Clip Tether60	412	4	1	2	3.99	4.940
No Clip Tether45	413	4	1	3	3.99	4.927
SingleComm Tether75	421	4	2	1	3.99	5.032
SingleComm Tether60	422	4	2	2	3.99	4.973
SingleComm Tether45	423	4	2	3	3.99	4.997
SingleCentral Tether75	431	4	3	1	3.99	5.063
SingleCentral Tether60	432	4	3	2	3.99	5.112
SingleCentral Tether45	433	4	3	3	3.99	5.095
DualCentral Tether75	441	4	4	1	3.99	4.930
DualCentral Tether60	442	4	4	2	3.99	5.097
DualCentral Tether45	443	4	4	3	3.99	5.175
CentralComm Tether75	451	4	5	1	3.99	4.958
CentralComm Tether60	452	4	5	2	3.99	4.938
CentralComm Tether45	453	4	5	3	3.99	5.075
No Clip Tether75	511	5	1	1	4.09	4.987
No Clip Tether60	512	5	1	2	4.09	4.956
No Clip Tether45	513	5	1	3	4.09	5.043
SingleComm Tether75	521	5	2	1	4.09	5.054
SingleComm Tether60	522	5	2	2	4.09	4.920
SingleComm Tether45	523	5	2	3	4.09	5.084
SingleCentral Tether75	531	5	3	1	4.09	4.928
SingleCentral Tether60	532	5	3	2	4.09	4.914
SingleCentral Tether45	533	5	3	3	4.09	4.983
DualCentral Tether75	541	5	4	1	4.09	4.956
DualCentral Tether60	542	5	4	2	4.09	4.948
DualCentral Tether45	543	5	4	3	4.09	5.030
CentralComm Tether75	551	5	5	1	4.09	5.046
CentralComm Tether60	552	5	5	2	4.09	4.939
CentralComm Tether45	553	5	5	3	4.09	5.124
No Clip Tether75	311	6	1	1	4.80	5.054
No Clip Tether60	312	6	1	2	4.80	5.007
No Clip Tether45	313	6	1	3	4.80	4.997
SingleComm Tether75	321	6	2	1	4.80	5.147
SingleComm Tether60	322	6	2	2	4.80	5.111
SingleComm Tether45	323	6	2	3	4.80	5.221
SingleCentral Tether75	331	6	3	1	4.80	5.052
SingleCentral Tether60	332	6	3	2	4.80	5.095
SingleCentral Tether45	333	6	3	3	4.80	5.068
DualCentral Tether75	341	6	4	1	4.80	5.106
DualCentral Tether60	342	6	4	2	4.80	5.119
DualCentral Tether45	343	6	4	3	4.80	5.155
CentralComm Tether75	351	6	5	1	4.80	5.136
CentralComm Tether60	352	6	5	2	4.80	5.176
CentralComm Tether45	353	6	5	3	4.80	5.115

A-9.4 Table Section B1

Gradients (mmHg)						
Peak Systolic	Mean Diastolic	Change from Baseline	Peak Diastolic	Change from Baseline	Moderate Stenosis?	Above 4 mmHg?
118.793	2.070		3.686		0	
119.598	2.875		4.662		0	
118.085	3.378		5.159		0	
122.138	3.479	1.409	5.511	1.825	0	0
119.542	3.341	0.466	5.322	0.660	0	0
121.944	5.722	2.344	8.893	3.734	1	1
121.350	4.189	2.119	6.861	3.175	0	1
121.330	4.397	1.522	7.257	2.595	0	1
120.960	5.815	2.437	9.172	4.013	1	1
120.549	4.277	2.207	7.314	3.628	0	1
118.611	4.855	1.980	8.133	3.471	0	1
121.591	5.764	2.386	9.811	4.652	1	1
119.616	4.334	2.264	7.625	3.939	0	1
118.551	4.509	1.634	7.864	3.202	0	1
121.057	6.050	2.672	10.288	5.129	1	1
119.943	0.791		2.217		0	
118.818	0.563		2.224		0	
120.076	2.495		4.125		0	
120.527	2.789		4.457	2.240	0	0
121.425	2.797		4.485	2.261	0	0
120.763	3.391	0.896	5.516	1.391	0	0
120.143	2.436		3.892	1.675	0	0
121.943	2.770		4.326	2.102	0	0
121.798	3.528	1.033	5.989	1.864	0	0
121.480	3.149		5.088	2.871	0	0
120.383	3.154		5.072	2.848	0	0
121.744	3.706	1.211	6.129	2.004	0	0
117.527	3.389		5.485	3.268	0	0
119.936	3.386		5.549	3.325	0	0
119.260	4.254	1.759	6.824	2.699	0	1
119.091	2.931		5.705		0	
119.328	2.864		5.551		0	
120.744	3.702		6.436		0	
119.417	3.280	0.349	5.513	-0.192	0	0
120.382	3.323	0.459	5.607	0.056	0	0
119.746	4.392	0.690	7.824	1.388	0	1
120.666	3.970	1.039	7.023	1.318	0	0
120.855	3.861	0.997	6.910	1.359	0	0
120.177	5.061	1.359	9.307	2.871	1	1
120.635	4.432	1.501	8.080	2.375	0	1
118.976	4.397	1.533	8.012	2.461	0	1
119.901	5.421	1.719	9.637	3.201	1	1
121.711	4.955	2.024	9.706	4.001	1	1
120.873	5.061	2.197	10.081	4.530	1	1
118.621	7.213		13.687	7.251	1	1

A-9.5 Table Section B2

120.859	2.565		5.147		0	
119.588	2.564		5.225		0	
122.194	3.060		5.545		0	
119.909	2.638	0.073	5.681	0.534	0	0
124.823	2.762	0.198	5.572	0.347	0	0
119.908	3.116	0.056	5.837	0.292	0	0
120.292	3.729	1.164	6.498	1.351	0	0
120.909	3.894	1.330	6.709	1.484	0	0
117.152	4.355	1.295	7.748	2.203	0	1
121.940	3.517	0.952	6.361	1.214	0	0
121.459	3.765	1.201	6.931	1.706	0	0
118.926	5.283	2.223	9.875	4.330	1	1
120.050	3.934	1.369	7.370	2.223	0	0
119.943	4.266	1.702	7.889	2.664	0	1
119.073	5.626	2.566	10.241	4.696	1	1
119.767	2.688		5.817		0	
120.981	2.761		5.877		0	
120.785	3.479		6.345		0	
120.660	3.024	0.336	6.406	0.589	0	0
120.728	3.005	0.244	6.304	0.427	0	0
119.853	3.335	-0.144	6.592	0.247	0	0
119.998	3.022	0.334	6.136	0.319	0	0
119.829	3.008	0.247	6.043	0.166	0	0
120.506	3.619	0.140	7.033	0.688	0	0
121.665	4.485	1.797	8.233	2.416	0	1
120.897	4.471	1.710	7.967	2.090	0	1
119.755	5.098	1.619	8.974	2.629	1	1
119.728	4.700	2.012	8.280	2.463	0	1
122.279	4.704	1.943	8.189	2.312	0	1
121.173	5.242	1.763	9.073	2.728	1	1
122.788	1.876		4.412		0	
124.108	1.870		4.778		0	
124.256	1.993		5.020		0	
121.681	2.177	0.301	4.745	0.333	0	0
122.702	2.165	0.295	4.846	0.067	0	0
121.890	2.598	0.605	5.411	0.391	0	0
121.712	2.261	0.385	5.036	0.624	0	0
122.678	2.421	0.551	5.155	0.376	0	0
123.965	2.886	0.894	5.755	0.735	0	0
121.707	2.854	0.978	5.524	1.112	0	0
121.901	2.731	0.861	5.205	0.426	0	0
121.969	3.414	1.421	6.217	1.197	0	0
120.608	3.220	1.344	6.046	1.635	0	0
120.630	3.203	1.334	5.935	1.156	0	0
122.953	3.863	1.870	7.401	2.381	0	0

A-9.6 Table Section C1

Mitral Valve Area (cm^2)							Fluid Force on MV (N)		
MVA 1	MVA 2	MVA 3	Mean MVA	Change from Baseline	SD MVA	DICOM Image	X Force	Y Force	Total Force
3.95	3.99	3.96	**3.97**		0.02	IM_0050	0.28	0.28	0.393
3.95	3.71	3.92	**3.86**		0.13	IM_0048	0.45	0.52	0.688
3.48	3.22	3.54	**3.41**		0.17	IM_0052	0.71	0.65	0.963
2.22	2.64	2.71	**2.52**	-1.443	0.27	IM_0073	0.71	0.18	0.730
2.39	2.32	2.37	**2.36**	-1.500	0.04	IM_0071	0.80	0.33	0.861
1.63	1.85	1.89	**1.79**	-1.623	0.14	IM_0069	1.17	0.36	1.225
2.41	2.27	2.38	**2.35**	-1.613	0.07	IM_0060	0.82	0.17	0.833
2.33	2.34	2.07	**2.25**	-1.613	0.15	IM_0058	0.92	0.31	0.971
1.82	1.80	1.57	**1.73**	-1.683	0.14	IM_0056	1.19	0.35	1.245
1.78	1.88	1.85	**1.84**	-2.130	0.05	IM_0066	0.95	0.14	0.964
1.75	1.54	1.63	**1.64**	-2.220	0.11	IM_0064	1.08	0.24	1.110
1.26	1.34	1.53	**1.38**	-2.037	0.14	IM_0062	1.28	0.29	1.315
1.55	1.50	1.39	**1.48**	-2.487	0.08	IM_0079	1.05	0.11	1.053
1.51	1.46	1.42	**1.46**	-2.397	0.05	IM_0077	1.10	0.22	1.125
1.27	1.23	1.37	**1.29**	-2.123	0.07	IM_0075	1.32	0.28	1.348
4.37	4.40	4.22	**4.33**		0.10	IM_0095	0.25	0.30	0.393
4.21	3.97	4.03	**4.07**		0.12	IM_0096	0.42	0.55	0.688
3.68	3.52	3.92	**3.71**		0.20	IM_0097	0.75	0.71	1.031
2.58	2.48	2.48	**2.51**	-1.817	0.06	IM_0106	0.80	0.18	0.824
2.39	2.21	2.32	**2.31**	-1.763	0.09	IM_0105	0.91	0.32	0.968
1.88	1.83	1.81	**1.84**	-1.867	0.04	IM_0104	1.14	0.37	1.202
2.98	2.86	2.82	**2.89**	-1.443	0.08	IM_0100	0.69	0.20	0.716
2.16	2.52	2.40	**2.36**	-1.710	0.18	IM_0099	0.89	0.33	0.951
1.84	1.88	1.94	**1.89**	-1.820	0.05	IM_0098	1.16	0.38	1.224
2.47	2.54	2.67	**2.56**	-1.770	0.10	IM_0103	0.83	0.18	0.850
2.23	2.33	2.15	**2.24**	-1.833	0.09	IM_0102	0.96	0.31	1.010
2.09	1.95	1.76	**1.93**	-1.773	0.17	IM_0101	1.16	0.39	1.227
1.95	1.73	1.80	**1.83**	-2.503	0.11	IM_0109	1.02	0.13	1.027
1.74	1.82	1.74	**1.77**	-2.303	0.05	IM_0108	1.08	0.25	1.111
1.50	1.50	1.49	**1.50**	-2.210	0.01	IM_0107	1.27	0.31	1.311
3.52	3.56	3.43	**3.50**		0.07	IM_0128	0.40	0.25	0.469
3.32	3.51	3.37	**3.40**		0.10	IM_0126	0.50	0.46	0.681
3.11	3.34	3.19	**3.21**		0.12	IM_0127	0.71	0.62	0.943
2.33	2.34	2.32	**2.33**	-1.173	0.01	IM_0141	0.66	0.17	0.682
2.20	2.36	2.24	**2.27**	-1.133	0.08	IM_0140	0.74	0.32	0.803
1.44	1.55	1.52	**1.50**	-1.710	0.06	IM_0138	1.06	0.31	1.106
2.51	2.58	2.29	**2.46**	-1.043	0.15	IM_0134	0.70	0.18	0.725
2.24	2.26	2.29	**2.26**	-1.137	0.03	IM_0133	0.80	0.31	0.861
1.43	1.53	1.41	**1.46**	-1.757	0.06	IM_0132	1.14	0.31	1.180
1.76	1.53	1.58	**1.62**	-1.880	0.12	IM_0137	0.94	0.12	0.948
1.47	1.86	1.60	**1.64**	-1.757	0.20	IM_0136	0.98	0.24	1.006
1.18	1.37	1.05	**1.20**	-2.013	0.16	IM_0135	1.19	0.27	1.222
1.37	1.41	1.28	**1.35**	-2.150	0.07	IM_0154	1.07	0.11	1.079
1.34	1.49	1.23	**1.35**	-2.047	0.13	IM_0153	1.13	0.20	1.149
1.01	0.92	1.03	**0.99**	-2.227	0.06	IM_0152	1.42	0.23	1.435

A-9.7 Table Section C2

3.70	3.92	3.78	**3.80**		0.11	IM_0160	0.42	0.26	0.498
3.58	3.60	3.51	**3.56**		0.05	IM_0158	0.57	0.48	0.747
3.22	3.42	3.50	**3.38**		0.14	IM_0159	0.76	0.65	1.000
2.41	2.30	2.21	**2.31**	-1.493	0.10	IM_0169	0.79	0.17	0.812
2.04	2.20	2.03	**2.09**	-1.473	0.10	IM_0168	0.89	0.29	0.939
1.87	1.96	1.79	**1.87**	-1.507	0.09	IM_0167	1.03	0.38	1.095
2.33	2.13	2.10	**2.19**	-1.613	0.13	IM_0163	0.86	0.16	0.879
1.78	1.99	1.92	**1.90**	-1.667	0.11	IM_0162	0.99	0.27	1.027
1.74	1.79	1.67	**1.73**	-1.647	0.06	IM_0161	1.15	0.35	1.205
1.81	1.91	1.91	**1.88**	-1.923	0.06	IM_0166	0.93	0.14	0.937
1.70	1.69	1.74	**1.71**	-1.853	0.03	IM_0165	1.04	0.25	1.068
1.41	1.55	1.51	**1.49**	-1.890	0.07	IM_0164	1.30	0.31	1.339
1.46	2.16	1.67	**1.76**	-2.037	0.36	IM_0172	1.00	0.13	1.013
1.36	1.34	1.27	**1.32**	-2.240	0.05	IM_0171	1.16	0.20	1.179
1.06	1.15	1.16	**1.12**	-2.257	0.06	IM_0170	1.37	0.25	1.398
3.81	3.99	4.05	**3.95**		0.12	IM_0188	0.46	0.28	0.533
3.80	3.91	3.79	**3.83**		0.07	IM_0189	0.58	0.52	0.779
3.38	3.54	3.61	**3.51**		0.12	IM_0190	0.82	0.67	1.057
1.89	1.97	1.98	**1.95**	-2.003	0.05	IM_0200	0.95	0.14	0.959
1.98	1.99	1.80	**1.92**	-1.910	0.11	IM_0199	1.00	0.27	1.035
1.54	1.57	1.54	**1.55**	-1.960	0.02	IM_0198	1.15	0.32	1.198
2.46	2.59	2.46	**2.50**	-1.447	0.08	IM_0193	0.81	0.18	0.828
2.24	2.31	2.25	**2.27**	-1.567	0.04	IM_0192	0.92	0.32	0.968
1.69	1.81	1.70	**1.73**	-1.777	0.07	IM_0191	1.15	0.35	1.202
1.86	1.69	1.85	**1.80**	-2.150	0.10	IM_0197	1.08	0.13	1.087
1.64	1.69	1.69	**1.67**	-2.160	0.03	IM_0196	1.14	0.24	1.163
1.41	1.47	1.30	**1.39**	-2.117	0.09	IM_0194	1.31	0.30	1.340
1.32	1.22	1.26	**1.27**	-2.683	0.05	IM_0203	1.19	0.10	1.197
1.21	1.20	1.19	**1.20**	-2.633	0.01	IM_0202	1.24	0.19	1.250
1.05	1.07	1.16	**1.09**	-2.417	0.06	IM_0201	1.35	0.25	1.378
4.70	4.59	4.73	**4.67**		0.07	IM_0204	0.44	0.32	0.544
4.55	4.52	4.39	**4.49**		0.09	IM_0205	0.62	0.60	0.861
4.19	4.24	4.32	**4.25**		0.07	IM_0206	0.85	0.81	1.172
3.60	3.70	3.56	**3.62**	-1.053	0.07	IM_0213	0.71	0.25	0.749
3.20	3.41	3.13	**3.25**	-1.240	0.15	IM_0214	0.88	0.44	0.984
2.77	2.48	2.72	**2.66**	-1.593	0.16	IM_0215	1.15	0.52	1.257
2.85	2.98	2.99	**2.94**	-1.733	0.08	IM_0207	0.88	0.21	0.905
2.35	2.24	2.40	**2.33**	-2.157	0.08	IM_0208	1.09	0.32	1.136
1.95	1.69	1.89	**1.84**	-2.407	0.14	IM_0209	1.30	0.37	1.354
2.49	2.41	2.40	**2.43**	-2.240	0.05	IM_0210	1.03	0.17	1.043
2.42	2.42	2.44	**2.43**	-2.060	0.01	IM_0211	1.07	0.34	1.123
1.60	1.69	1.67	**1.65**	-2.597	0.05	IM_0212	1.36	0.34	1.403
1.87	1.62	1.99	**1.83**	-2.847	0.19	IM_0216	1.20	0.13	1.205
1.87	2.01	1.77	**1.88**	-2.603	0.12	IM_0217	1.23	0.27	1.256
1.23	1.18	1.11	**1.17**	-3.077	0.06	IM_0218	1.51	0.26	1.531

APPENDIX B. ENGINEERING DRAWINGS

B-1 Adjustable Annulus Plate Engineering Drawing

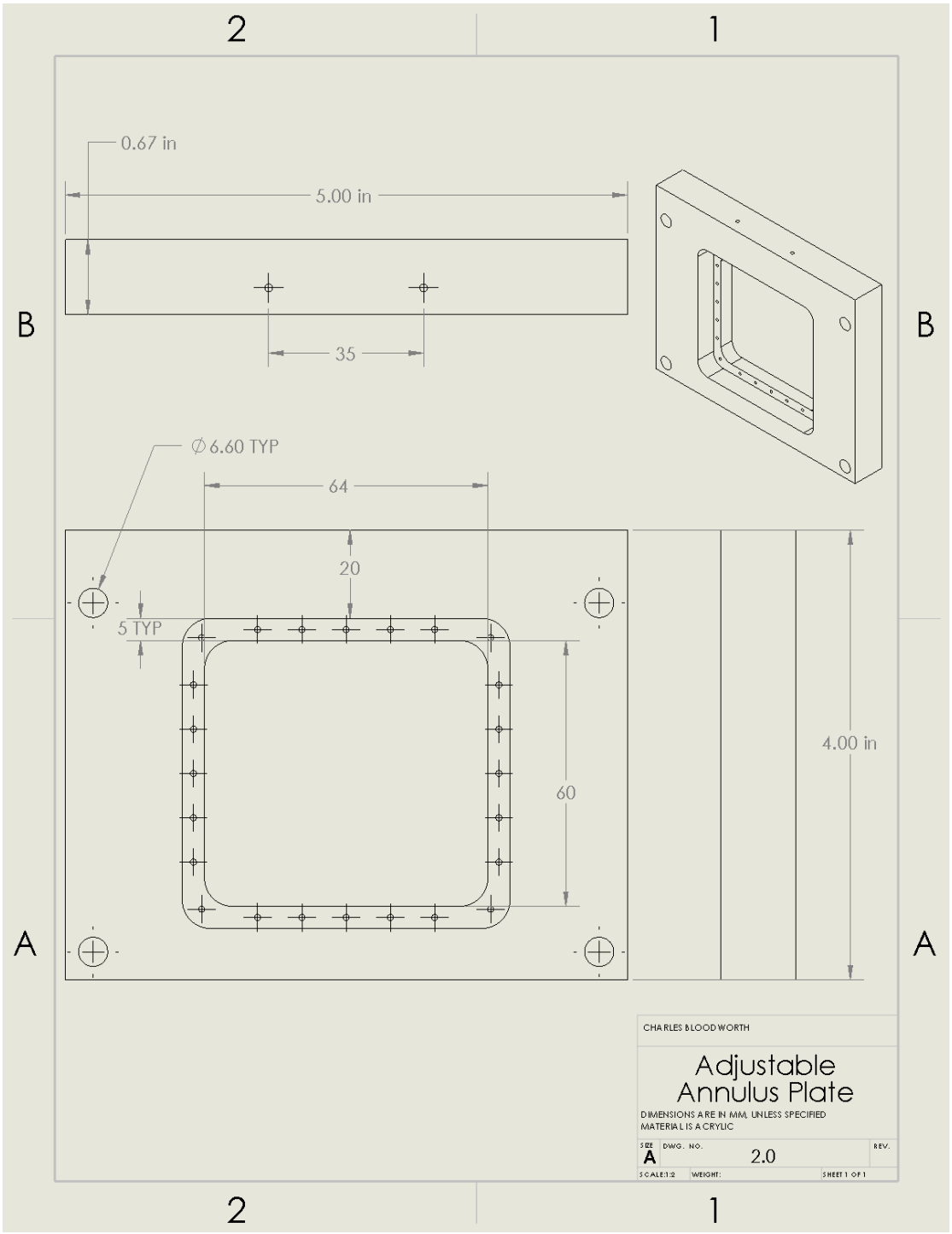

B-2 GTclip Engineering Drawing

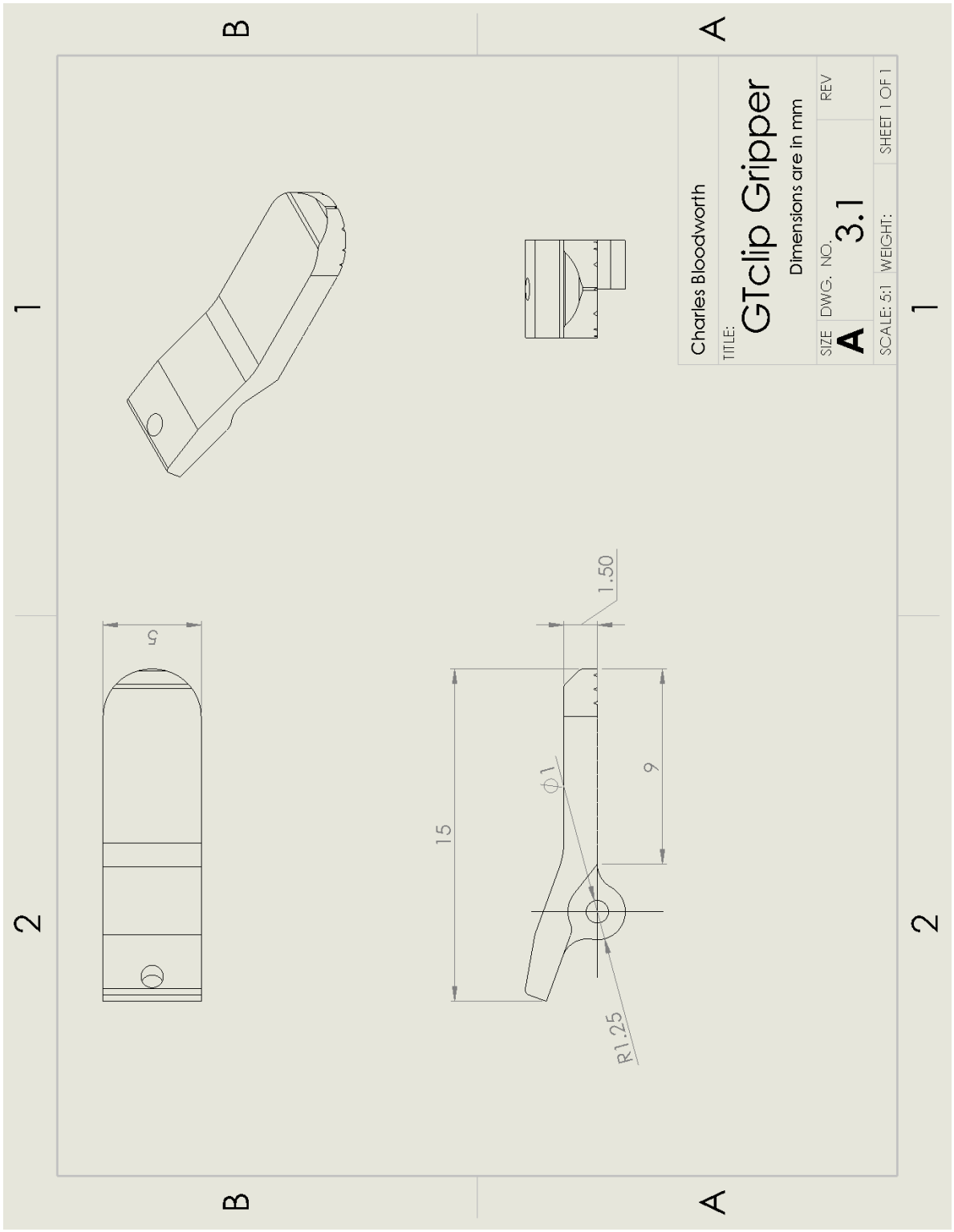

B-3 GT Left Heart Simulator Ventricle Engineering Drawing

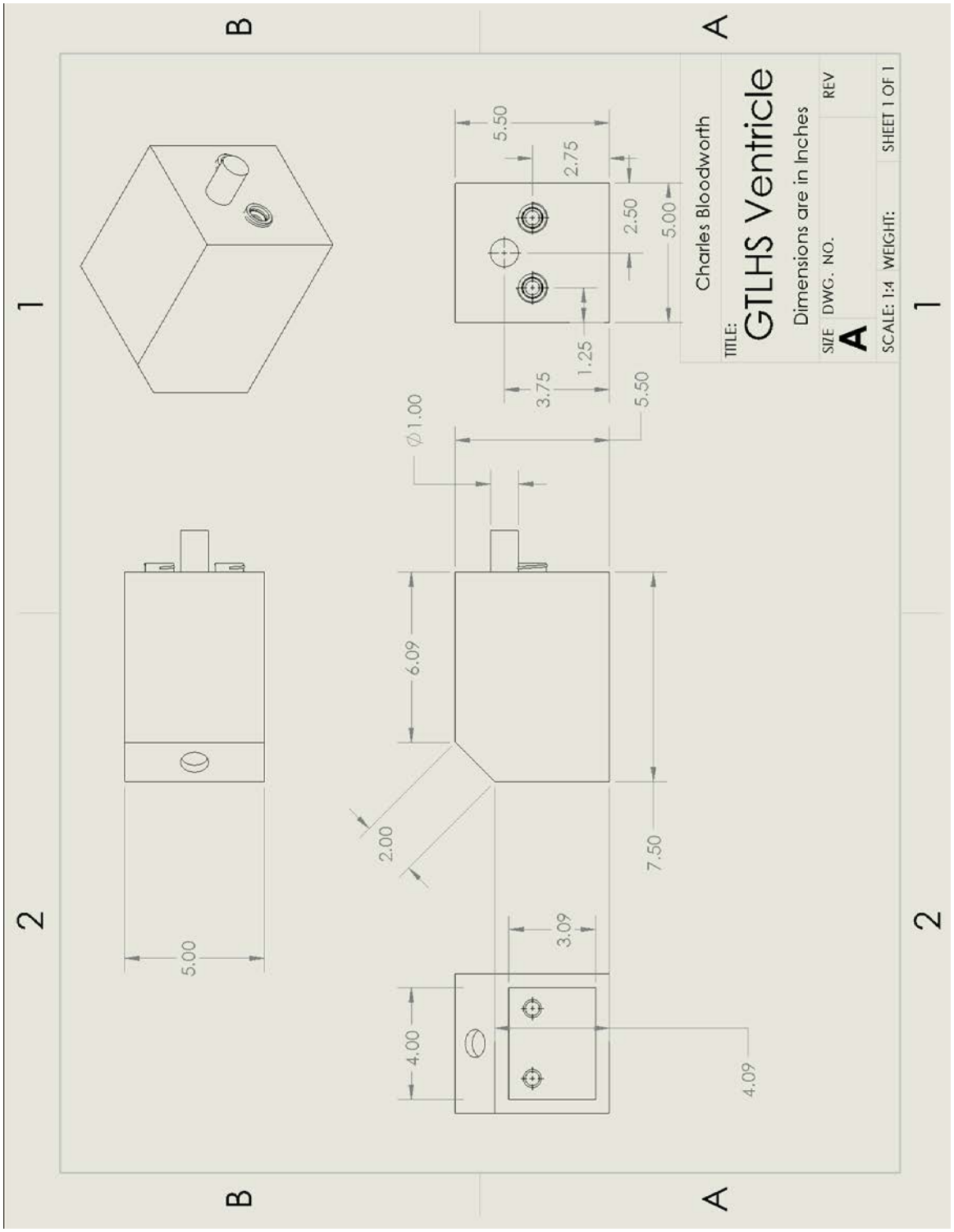

B-4 GT Left Heart Simulator Atrium Engineering Drawing

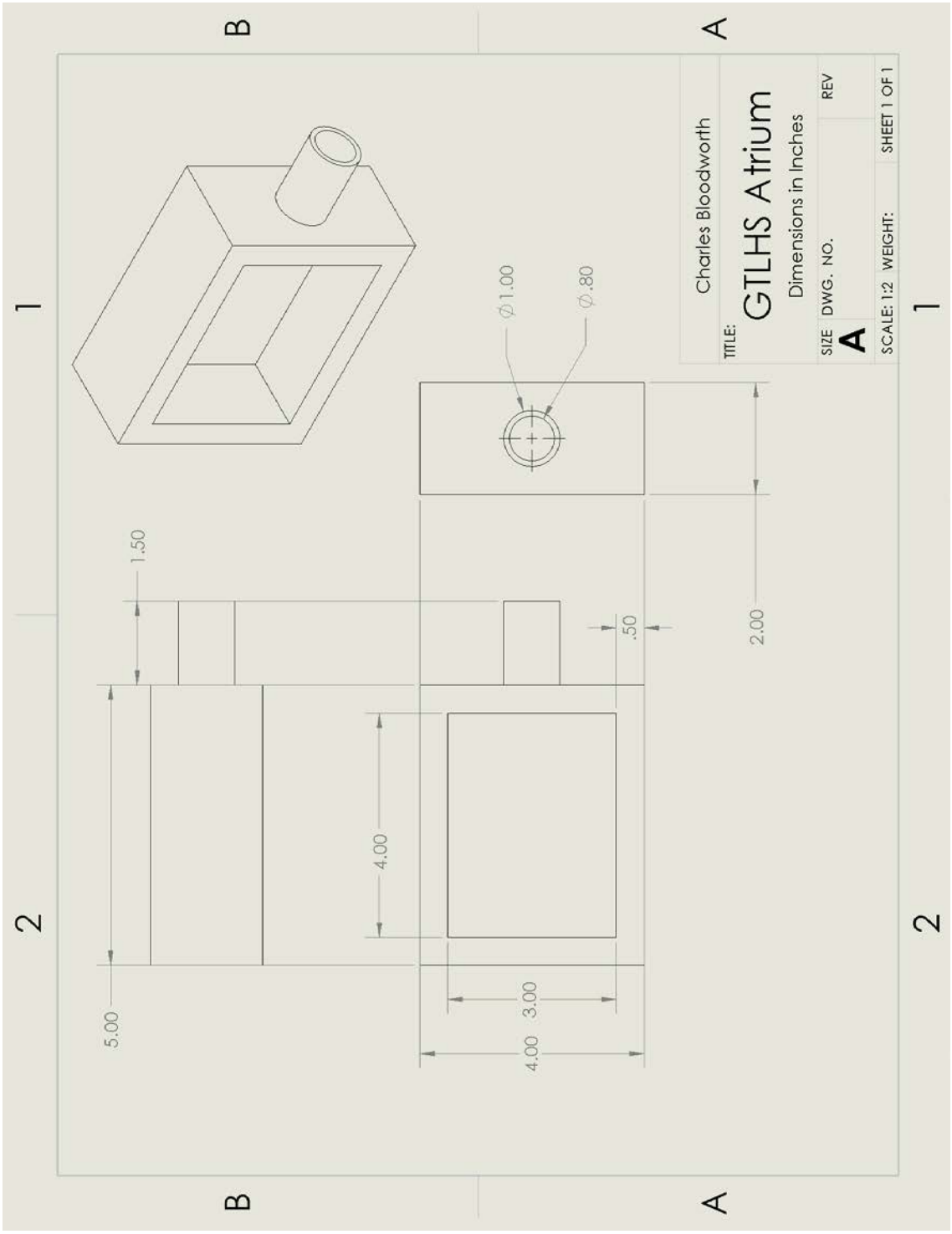

APPENDIX C. CATALOG OF DATA STORAGE

C.1 General Manuals and Guides

The following documents are stored under:

\yogi-lab\CFM Transitions\Charlie Transition\MANUALS AND GUIDES

\Loop Setup and Operation

GT left *and* right heart simulator setup and tuning, target hemodynamics, loop configuration.

\MV Excision and Mounting

Animal mitral valve excision, prep, annulus suturing, papillary muscle prep and fixturing

\MicroCT Prep and Scanning

Scanning mounted mitral valve samples by MicroCT unloaded, glutaraldehyde fixed, and under steady pressure.

\Heartbeater User Guide

Setup, operation and troubleshooting of the LabVIEW VI that controls GT heart simulators.

C.2 Thesis Documents and Data

The following documents are stored under:

\yogi-lab\CFM Transitions\Charlie Transition\THESIS

\CAD

\GTclip

CAD, CAM and bill of materials for GTclip.

\Square Adjustable Annulus

CAD, CAM and bill of materials for the square adjustable annulus.

\Data

\Hemo

Contains all hemo recordings gathered for the MitraClip experiments.

\Summarized Final Data

Contains master spreadsheet of all final data used in thesis project, along with bar graphs. MATLAB programs and Minitab files are also included.

The library of all echo images can be found on AadiBozz under yogi-lab\Mitral Valve Group - Everything\Experimental Data\MitraClip_CHB

\Dissertation Document

All files, figures and documents pertaining to the thesis dissertation document, including the final, approved document.

\Figures and Images

All figures, images and videos made pertaining to the MitraClip experiments. Videos are included in GIF format.

\Literature

Important papers and literature. Additional papers can be found in the references section of the thesis dissertation

\Presentation Slides

Library of all slides and presentations made for the MitraClip project.

\Publication – JACC Intervention 2017

Figures and manuscripts related to submitted publication for this work.

REFERENCES

1. Iung B and Vahanian A. Epidemiology of acquired valvular heart disease. *Can J Cardiol*. 2014;30:962-70.

2. Nkomo VT, Gardin JM, Skelton TN, Gottdiener JS, Scott CG and Enriquez-Sarano M. Burden of valvular heart diseases: a population-based study. *Lancet*. 2006;368:1005-11.

3. Carpentier A, Adams DH and Filsoufi F. *Carpentier's reconstructive valve surgery*: Elsevier Health Sciences; 2011.

4. Hung J, Papakostas L, Tahta SA, Hardy BG, Bollen BA, Duran CM and Levine RA. Mechanism of recurrent ischemic mitral regurgitation after annuloplasty: continued LV remodeling as a moving target. *Circulation*. 2004;110:II85-90.

5. Borger MA, Alam A, Murphy PM, Doenst T and David TE. Chronic ischemic mitral regurgitation: repair, replace or rethink? *Ann Thorac Surg*. 2006;81:1153-61.

6. Vergnat M, Jassar AS, Jackson BM, Ryan LP, Eperjesi TJ, Pouch AM, Weiss SJ, Cheung AT, Acker MA, Gorman JH and Gorman RC. Ischemic Mitral Regurgitation: A Quantitative Three-Dimensional Echocardiographic Analysis. *Annals of Thoracic Surgery*. 2011;91:157-164.

7. Sorajja P, Leon MB, Adams DH, Webb JG and Farivar RS. Transcatheter Therapy for Mitral Regurgitation Clinical Challenges and Potential Solutions. *Circulation*. 2017;136:404-417.

8. Braunberger E, Deloche A, Berrebi A, Abdallah F, Celestin JA, Meimoun P, Chatellier G, Chauvaud S, Fabiani JN and Carpentier A. Very long-term results (more than 20 years) of valve repair with carpentier's techniques in nonrheumatic mitral valve insufficiency. *Circulation*. 2001;104:I8-11.

9. De Bonis M, Ferrara D, Taramasso M, Calabrese MC, Verzini A, Buzzatti N and Alfieri O. Mitral replacement or repair for functional mitral regurgitation in dilated and ischemic cardiomyopathy: is it really the same? *Ann Thorac Surg*. 2012;94:44-51.

10. Gillinov AM, Wierup PN, Blackstone EH, Bishay ES, Cosgrove DM, White J, Lytle BW and McCarthy PM. Is repair preferable to replacement for ischemic mitral regurgitation? *J Thorac Cardiovasc Surg*. 2001;122:1125-41.

11. Kuwahara E, Otsuji Y, Iguro Y, Ueno T, Zhu F, Mizukami N, Kubota K, Nakashiki K, Yuasa T, Yu B, Uemura T, Takasaki K, Miyata M, Hamasaki S, Kisanuki A, Levine RA, Sakata R and Tei C. Mechanism of recurrent/persistent ischemic/functional mitral regurgitation in the chronic phase after surgical annuloplasty: importance of augmented posterior leaflet tethering. *Circulation*. 2006;114:I529-34.

12. Fucci C, Sandrelli L, Pardini A, Torracca L, Ferrari M and Alfieri O. Improved results with mitral valve repair using new surgical techniques. *Eur J Cardiothorac Surg*. 1995;9:621-6 discuss 626-7.

13. Alfieri O, Maisano F, De Bonis M, Stefano PL, Torracca L, Oppizzi M and La Canna G. The double-orifice technique in mitral valve repair: a simple solution for complex problems. *J Thorac Cardiovasc Surg*. 2001;122:674-81.

14. De Bonis M and Alfieri O. The edge-to-edge technique for mitral valve repair. *HSR Proc Intensive Care Cardiovasc Anesth*. 2010;2:7-17.

15. Feldman T, Kar S, Rinaldi M, Fail P, Hermiller J, Smalling R, Whitlow PL, Gray W, Low R, Herrmann HC, Lim S, Foster E, Glower D and Investigators E. Percutaneous mitral repair with the MitraClip system: safety and midterm durability in the initial EVEREST (Endovascular Valve Edge-to-Edge REpair Study) cohort. *J Am Coll Cardiol*. 2009;54:686-94.

16. Rogers JH and Franzen O. Percutaneous edge-to-edge MitraClip therapy in the management of mitral regurgitation. *Eur Heart J*. 2011;32:2350-7.

17. Mirabel M, Iung B, Baron G, Messika-Zeitoun D, Detaint D, Vanoverschelde JL, Butchart EG, Ravaud P and Vahanian A. What are the characteristics of patients with severe, symptomatic, mitral regurgitation who are denied surgery? *Eur Heart J*. 2007;28:1358-65.

18. St Goar FG, Fann JI, Komtebedde J, Foster E, Oz MC, Fogarty TJ, Feldman T and Block PC. Endovascular edge-to-edge mitral valve repair: short-term results in a porcine model. *Circulation*. 2003;108:1990-3.

19. Feldman T, Foster E, Glower DD, Kar S, Rinaldi MJ, Fail PS, Smalling RW, Siegel R, Rose GA, Engeron E, Loghin C, Trento A, Skipper ER, Fudge T, Letsou GV, Massaro JM, Mauri L and Investigators EI. Percutaneous repair or surgery for mitral regurgitation. *N Engl J Med*. 2011;364:1395-406.

20. Nishimura RA, Otto CM, Bonow RO, Carabello BA, Erwin JP, 3rd, Guyton RA, O'Gara PT, Ruiz CE, Skubas NJ, Sorajja P, Sundt TM, 3rd, Thomas JD and Members AATF. 2014 AHA/ACC Guideline for the Management of Patients With Valvular Heart Disease: a report of the American College of Cardiology/American Heart Association Task Force on Practice Guidelines. *Circulation*. 2014;129:e521-643.

21. Adamo M, Chiari E, Curello S, Maiandi C, Chizzola G, Fiorina C, Frontini M, Cuminetti G, Pezzotti E, Rovetta R, Lombardi CM, Manzato A, Metra M and Ettori F. Mitraclip therapy in patients with functional mitral regurgitation and missing leaflet coaptation: is it still an exclusion criterion? *Eur J Heart Fail*. 2016;18:1278-1286.

22. Feldman T, Kar S, Elmariah S, Smart SC, Trento A, Siegel RJ, Apruzzese P, Fail P, Rinaldi MJ, Smalling RW, Hermiller JB, Heimansohn D, Gray WA, Grayburn PA, Mack MJ, Lim DS, Ailawadi G, Herrmann HC, Acker MA, Silvestry FE, Foster E, Wang A,

Glower DD, Mauri L and Investigators EI. Randomized Comparison of Percutaneous Repair and Surgery for Mitral Regurgitation: 5-Year Results of EVEREST II. *J Am Coll Cardiol*. 2015;66:2844-54.

23. Franzen O, Baldus S, Rudolph V, Meyer S, Knap M, Koschyk D, Treede H, Barmeyer A, Schofer J, Costard-Jackle A, Schluter M, Reichenspurner H and Meinertz T. Acute outcomes of MitraClip therapy for mitral regurgitation in high-surgical-risk patients: emphasis on adverse valve morphology and severe left ventricular dysfunction. *Eur Heart J*. 2010;31:1373-81.

24. Kische S, Nienaber C and Ince H. Use of four MitraClip devices in a patient with ischemic cardiomyopathy and mitral regurgitation: "zipping by clipping". *Catheter Cardiovasc Interv*. 2012;80:1007-13.

25. Cilingiroglu M. Mitral stenosis following MitraClip procedure: is it preventable? *Catheter Cardiovasc Interv*. 2014;83:303-4.

26. Bhattacharya S and He Z. Mechanics of mitral valve edge-to-edge-repair and MitraClip procedure. *J Long Term Eff Med Implants*. 2015;25:135-45.

27. Rabbah JP, Siefert AW, Spinner EM, Saikrishnan N and Yoganathan AP. Peak mechanical loads induced in the in vitro edge-to-edge repair of posterior leaflet flail. *Ann Thorac Surg*. 2012;94:1446-53.

28. Jimenez JH, Forbess J, Croft LR, Small L, He Z and Yoganathan AP. Effects of annular size, transmitral pressure, and mitral flow rate on the edge-to-edge repair: an in vitro study. *Ann Thorac Surg*. 2006;82:1362-8.

29. Croft LR, Jimenez JH, Gorman RC, Gorman JH, 3rd and Yoganathan AP. Efficacy of the edge-to-edge repair in the setting of a dilated ventricle: an in vitro study. *Ann Thorac Surg*. 2007;84:1578-84.

30. Jimenez JH, Liou SW, Padala M, He Z, Sacks M, Gorman RC, Gorman JH, 3rd and Yoganathan AP. A saddle-shaped annulus reduces systolic strain on the central region of the mitral valve anterior leaflet. *J Thorac Cardiovasc Surg*. 2007;134:1562-8.

31. Nielsen SL, Timek TA, Lai DT, Daughters GT, Liang D, Hasenkam JM, Ingels NB and Miller DC. Edge-to-edge mitral repair: tension on the approximating suture and leaflet deformation during acute ischemic mitral regurgitation in the ovine heart. *Circulation*. 2001;104:I29-35.

32. Timek TA, Nielsen SL, Lai DT, Tibayan F, Liang D, Daughters GT, Beineke P, Hastie T, Ingels NB, Jr. and Miller DC. Mitral annular size predicts Alfieri stitch tension in mitral edge-to-edge repair. *J Heart Valve Dis*. 2004;13:165-73.

33. Sturla F, Vismara R, Jaworek M, Votta E, Romitelli P, Pappalardo OA, Lucherini F, Antona C, Fiore GB and Redaelli A. In vitro and in silico approaches to quantify the effects of the Mitraclip(R) system on mitral valve function. *J Biomech*. 2017;50:83-92.

34. Lau KD, Diaz-Zuccarini V, Scambler P and Burriesci G. Fluid-structure interaction study of the edge-to-edge repair technique on the mitral valve. *J Biomech*. 2011;44:2409-17.

35. Kunzelman KS, Reimink MS and Cochran RP. Flexible versus rigid ring annuloplasty for mitral valve annular dilatation: a finite element model. *J Heart Valve Dis*. 1998;7:108-16.

36. Kunzelman KS, Reimink MS and Cochran RP. Annular dilatation increases stress in the mitral valve and delays coaptation: a finite element computer model. *Cardiovasc Surg*. 1997;5:427-34.

37. Kunzelman K, Reimink MS, Verrier ED and Cochran RP. Replacement of mitral valve posterior chordae tendineae with expanded polytetrafluoroethylene suture: a finite element study. *J Card Surg*. 1996;11:136-45; discussion 146.

38. Votta E, Maisano F, Soncini M, Redaelli A, Montevecchi FM and Alfieri O. 3-D computational analysis of the stress distribution on the leaflets after edge-to-edge repair of mitral regurgitation. *J Heart Valve Dis*. 2002;11:810-22.

39. Votta E, Caiani E, Veronesi F, Soncini M, Montevecchi FM and Redaelli A. Mitral valve finite-element modelling from ultrasound data: a pilot study for a new approach to understand mitral function and clinical scenarios. *Philos Trans A Math Phys Eng Sci*. 2008;366:3411-34.

40. Feldman T and Guerrero M. Assessing the Balance Between Less Mitral Regurgitation and More Residual Transmitral Pressure Gradient After MitraClip. *JACC Cardiovasc Interv*. 2017;10:940-941.

41. Cockburn J, Fragkou P and Hildick-Smith D. Development of mitral stenosis after single MitraClip insertion for severe mitral regurgitation. *Catheter Cardiovasc Interv*. 2014;83:297-302.

42. Neuss M, Schau T, Isotani A, Pilz M, Schopp M and Butter C. Elevated Mitral Valve Pressure Gradient After MitraClip Implantation Deteriorates Long-Term Outcome in Patients With Severe Mitral Regurgitation and Severe Heart Failure. *JACC Cardiovasc Interv*. 2017;10:931-939.

43. Lim DS, Reynolds MR, Feldman T, Kar S, Herrmann HC, Wang A, Whitlow PL, Gray WA, Grayburn P, Mack MJ and Glower DD. Improved functional status and quality of life in prohibitive surgical risk patients with degenerative mitral regurgitation after transcatheter mitral valve repair. *J Am Coll Cardiol*. 2014;64:182-92.

44. Singh GD, Smith TW and Rogers JH. Multi-MitraClip therapy for severe degenerative mitral regurgitation: "anchor" technique for extremely flail segments. *Catheter Cardiovasc Interv*. 2015;86:339-46.

45. Baumgartner H, Hung J, Bermejo J, Chambers JB, Evangelista A, Griffin BP, Iung B, Otto CM, Pellikka PA, Quinones M, American Society of E and European Association of E. Echocardiographic assessment of valve stenosis: EAE/ASE recommendations for clinical practice. *J Am Soc Echocardiogr*. 2009;22:1-23; quiz 101-2.

46. Herrmann HC, Kar S, Siegel R, Fail P, Loghin C, Lim S, Hahn R, Rogers JH, Bommer WJ, Wang A, Berke A, Lerakis S, Kramer P, Wong SC, Foster E, Glower D, Feldman T and Investigators E. Effect of percutaneous mitral repair with the MitraClip device on mitral valve area and gradient. *EuroIntervention*. 2009;4:437-42.

47. Otsuji Y, Gilon D, Jiang L, He S, Leavitt M, Roy MJ, Birmingham MJ and Levine RA. Restricted diastolic opening of the mitral leaflets in patients with left ventricular dysfunction: evidence for increased valve tethering. *J Am Coll Cardiol*. 1998;32:398-404.

48. Chan PH, She HL, Alegria-Barrero E, Moat N, Di Mario C and Franzen O. Real-world experience of MitraClip for treatment of severe mitral regurgitation. *Circ J*. 2012;76:2488-93.

49. Kubota K, Otsuji Y, Ueno T, Koriyama C, Levine RA, Sakata R and Tei C. Functional mitral stenosis after surgical annuloplasty for ischemic mitral regurgitation: importance of subvalvular tethering in the mechanism and dynamic deterioration during exertion. *J Thorac Cardiovasc Surg*. 2010;140:617-23.

50. Siefert AW, Rabbah JP, Koomalsingh KJ, Touchton SA, Jr., Saikrishnan N, McGarvey JR, Gorman RC, Gorman JH, 3rd and Yoganathan AP. In vitro mitral valve simulator mimics systolic valvular function of chronic ischemic mitral regurgitation ovine model. *Ann Thorac Surg*. 2013;95:825-30.

51. Bloodworth CHt, Pierce EL, Easley TF, Drach A, Khalighi AH, Toma M, Jensen MO, Sacks MS and Yoganathan AP. Ex Vivo Methods for Informing Computational Models of the Mitral Valve. *Ann Biomed Eng*. 2017;45:496-507.

52. Rabbah JP, Siefert AW, Bolling SF and Yoganathan AP. Mitral valve annuloplasty and anterior leaflet augmentation for functional ischemic mitral regurgitation: quantitative comparison of coaptation and subvalvular tethering. *J Thorac Cardiovasc Surg*. 2014;148:1688-93.

53. Alozie A, Westphal B, Kische S, Kaminski A, Paranskaya L, Bozdag-Turan I, Ortak J, Schubert J, Steinhoff G and Ince H. Surgical revision after percutaneous mitral valve repair by edge-to-edge device: when the strategy fails in the highest risk surgical population. *Eur J Cardiothorac Surg*. 2014;46:55-60.

54. Alegria-Barrero E, Chan PH, Foin N, Syrseloudis D, Tavazzi G, Price S, Lindsay AC, Duncan A, Moat N, Di Mario C and Franzen OW. Concept of the central clip: when to use one or two MitraClips(R). *EuroIntervention*. 2014;9:1217-24.

55. Estevez-Loureiro R, Franzen O, Winter R, Sondergaard L, Jacobsen P, Cheung G, Moat N, Ihlemann N, Ghione M, Price S, Duncan A, Streit Rosenberg T, Barker S, Di

Mario C and Settergren M. Echocardiographic and clinical outcomes of central versus noncentral percutaneous edge-to-edge repair of degenerative mitral regurgitation. *J Am Coll Cardiol*. 2013;62:2370-7.

56. Biaggi P, Felix C, Gruner C, Herzog BA, Hohlfeld S, Gaemperli O, Stahli BE, Paul M, Held L, Tanner FC, Grunenfelder J, Corti R and Bettex D. Assessment of mitral valve area during percutaneous mitral valve repair using the MitraClip system: comparison of different echocardiographic methods. *Circ Cardiovasc Imaging*. 2013;6:1032-40.

57. Fox RW, McDonald AT and Pritchard PJ. *Introduction to fluid mechanics*: John Wiley & Sons New York; 1998.

58. Sturla F, Redaelli A, Puppini G, Onorati F, Faggian G and Votta E. Functional and Biomechanical Effects of the Edge-to-Edge Repair in the Setting of Mitral Regurgitation: Consolidated Knowledge and Novel Tools to Gain Insight into Its Percutaneous Implementation. *Cardiovasc Eng Technol*. 2015;6:117-40.

59. Rabbah JP, Chism B, Siefert A, Saikrishnan N, Veledar E, Thourani VH and Yoganathan AP. Effects of targeted papillary muscle relocation on mitral leaflet tenting and coaptation. *Ann Thorac Surg*. 2013;95:621-8.

60. Lazar HL. Mitral Stenosis Following Mitral Valve Repair For Degenerative Mitral Regurgitation—Lessons Learned. 2017.

61. Alfieri O and Denti P. Alfieri stitch and its impact on mitral clip. *Eur J Cardiothorac Surg*. 2011;39:807-8.

62. Kapadia S, Krishnaswamy A and Tuzcu EM. Percutaneous Therapy for Tricuspid Regurgitation: A New Frontier for Interventional Cardiology. *Circulation*. 2017;135:1815-1818.

63. Geidel S and Schmoeckel M. Impact of failed mitral clipping on subsequent mitral valve operations. *Ann Thorac Surg*. 2014;97:56-63.

64. Vismara R, Gelpi G, Prabhu S, Romitelli P, Troxler LG, Mangini A, Romagnoni C, Contino M, Van Hoven DT, Lucherini F, Jaworek M, Redaelli A, Fiore GB and Antona C. Transcatheter Edge-to-Edge Treatment of Functional Tricuspid Regurgitation in an Ex Vivo Pulsatile Heart Model. *J Am Coll Cardiol*. 2016;68:1024-33.